AD-A016 786

AFRPL GRAPHITE PERFORMANCE PREDICTION PPOGRAM. VOLUME II. ARC PLASMA GENERATOR EVALUATION OF GRAPHITE REACTION KINETICS IN ROCKET PROPELLANT ENVIRONMENTS

H. Tong, et al

Acurex Corporation

Prepared for:

Air Force Rocket Propulsion Laboratory

October 1975

DISTRIBUTED BY:

NTIS

National Technical Information Service
U. S. DEPARTMENT OF COMMERCE

315130

AFRPL-TR-75-59

AEROTHERM PROJECT 7113
AEROTHERM REPORT NO. 75-143

AFRPL GRAPHITE PERFORMANCE PREDICTION PROGRAM

INTERIM REPORT

VOLUME II. ARC PLASMA GENERATOR EVALUATION OF GRAPHITE REACTION KINETICS IN ROCKET PROPELLANT ENVIRONMENTS

AD A016786

AEROTHERM DIVISION/ACUREX CORPORATION
485 CLYDE AVENUE
MOUNTAIN VIEW, CALIFORNIA 94042

AUTHORS: H. TONG
J.C. HARTMAN
E. K. CHU

OCTOBER 1975

APPROVED FOR PUBLIC RELEASE:
DISTRIBUTION UNLIMITED

AIR FORCE ROCKET PROPULSION LABORATORY
DIRECTOR OF SCIENCE AND TECHNOLOGY
AIR FORCE SYSTEMS COMMAND
EDWARDS, CA 93523

UNCLASSIFIED
SECURITY CLASSIFICATION OF THIS PAGE (When Data Entered)

REPORT DOCUMENTATION PAGE

READ INSTRUCTIONS BEFORE COMPLETING FORM

1. REPORT NUMBER: AFRPL-TR-75-59
2. GOVT ACCESSION NO.:
3. RECIPIENT'S CATALOG NUMBER:

4. TITLE (and Subtitle): AFRPL GRAPHITE PERFORMANCE PREDICTION
Vol II Arc Plasma Generator Evaluation of Graphite Reaction Kinetics in Rkt Propellant Environments

5. TYPE OF REPORT & PERIOD COVERED: Interim Report May 1974 to May 1975
6. PERFORMING ORG. REPORT NUMBER:

7. AUTHOR(s): H. Tong, J.C. Hartman, E. K. Chu
8. CONTRACT OR GRANT NUMBER(s): F04611-74-C-0023

9. PERFORMING ORGANIZATION NAME AND ADDRESS: Aerotherm/Acurex Corporation, 485 Clyde Avenue, Mountain View, CA 94042
10. PROGRAM ELEMENT, PROJECT, TASK AREA & WORK UNIT NUMBERS: Project No. 6230F, BPSN: 305909HU

11. CONTROLLING OFFICE NAME AND ADDRESS: Air Force Rocket Propulsion Laboratory/MK, Edwards, CA 93523
12. REPORT DATE: October 1975
13. NUMBER OF PAGES: 69

14. MONITORING AGENCY NAME & ADDRESS (if different from Controlling Office):
15. SECURITY CLASS. (of this report): UNCLASSIFIED
15a. DECLASSIFICATION/DOWNGRADING SCHEDULE:

16. DISTRIBUTION STATEMENT (of this Report)
APPROVED FOR PUBLIC RELEASE; DISTRIBUTION UNLIMITED

17. DISTRIBUTION STATEMENT (of the abstract entered in Block 20, if different from Report)

18. SUPPLEMENTARY NOTES

19. KEY WORDS (Continue on reverse side if necessary and identify by block number)
Rocket Nozzle
Carbon
Graphite
Pyrolytic Graphite
Reaction Kinetics
Ablation Analysis
Surface Thermochemistry
Heat Transfer
Boundary Layer Analysis
ARC plasma generator

20. ABSTRACT (Continue on reverse side if necessary and identify by block number)
Test gases and conditions were selected for use in the arc plasma generation simulation of advanced propellant environments. Calibration and checkout results are reported. The experimental program to determine kinetic reaction rates of carbon and graphite materials will now proceed and be completed in early 1976.

DD FORM 1 JAN 73 1473 EDITION OF 1 NOV 65 IS OBSOLETE

UNCLASSIFIED
SECURITY CLASSIFICATION OF THIS PAGE (When Data Entered)

TABLE OF CONTENTS

LIST OF ILLUSTRATIONS

LIST OF TABLES

SECTION 1

INTRODUCTION

Because it is not possible to write an analytical expression which exactly models the real events associated with carbon consumption in rocket nozzles, one must resort to developing engineering approximations which represent the overall observed phenomena. Expressions of this type with a set of empirical coefficients were developed in Reference 1. The empirical coefficients relate the local thermochemical state to the surface temperature and carbon consumption rates. Thus, given an accurate set of data with these variables known, it is possible to write a kinetic equation for analytic prediction of ablation rates.

There are two viable experiments that can be conducted to obtain ablation data. First and certainly the most relevant is to fire actual rocket motors. Difficulties associated with this approach are:

1. Surface temperature is not a measured variable and can be experimentally adjusted only over a small range.
2. It is not possible to isolate even simple reactions to simplify the data analysis procedure.
3. Chamber conditions may vary widely during the ablation run.
4. The surface is subjected to an unknown quantity of ambient air oxidation during cooldown.
5. Heat transfer rate is not an easily controllable parameter nor can it be independently measured.
6. Rocket nozzles, in order to be structurally sound, are complex and may result in a variety of flow-disturbing features such as steps and gaps.
7. Motor firings are high-cost experiments.

The obvious advantage of motor data is that there is an exact simulation of the environment and material response.

The second approach is to conduct laboratory scale ablation measurements in prescribed simulation environments. Here, one has the option of selecting from a large number of potential experiments which range from heated filaments to miniature

nozzles heated in an arc plasma generator (APG) The latter was selected because it provides a good compromise between "academic' quality data and rocket motor data. The disadvantages of this and most laboratory tests are:

1. Surface temperatures and system pressures are less than those experienced in rocket motors.
2. The experiment must be viewed carefully to determine if test is kinetically or diffusively limited or somewhere in between.
3. Full-size components cannot be tested.
4. Some analytical technique must be available to sort out the effect of various reactants and to scale for predicting full-size performance.

The obvious advantage of a laboratory experiment is that one can obtain detailed measurements in a controlled environment. This data provides a separation of the effect of each constituent and yields temperature dependent reaction rates. In addition a large number of laboratory tests can be conducted at the cost of one motor firing.

Laboratory data and motor firing data are both important in the development of an accurate analysis procedure and should therefore be treated as being complimentary rather than competitive. In the current study, the complimentary aspects are being exploited wherever sufficient motor data are available. Laboratory data are being obtained in an arc plasma generator (APG) and are being analyzed simultaneously with motor recession rates which are analyzed and manipulated to look like APG data. Since the final analysis treats motor data and APG data as a single set of data, it is not possible to unequivocally define the function of each. However, in a loose general sense, an APG provides a large data base which allows a separation of the effect of various constituents or reactants whereas motor data provides high temperature, high pressure data points which make the analysis simultaneously relevant and accurate. The analysis procedure has been described elsewhere and will not be considered here.

The Aerotherm 1-megawatt arc plasma generator is a versatile test facility for determining the response of materials to hyperthermal environments. This facility has been used extensively for the evaluation of space shuttle and reentry vehicle thermal protection systems and rocket nozzle liner materials. Air and inert gases such as argon and helium are common gases to pass through the arc heater and are usually sufficient for simulating earth entry conditions. However, in a rocket nozzle, a substantial constituent is hydrogen and proper simulation and separation of kinetic events requires that hydrogen be used in the arc plasma generator. The Aerotherm arc plasma facility is unique in this regard since it is one of the few arc plasma facilities in the country that uses hydrogen gas routinely.

This report will describe the facility and its application to the determination of kinetic reaction rates for graphitic rocket nozzle materials.

SECTION 2

EXPERIMENTAL APPARATUS

The experimental apparatus consists of the arc plasma generator used to produce the high temperature reactive environments, the test nozzles which are exposed to these environments, the fume collection, cooling and scrubbing system used to remove the test gases from the facility, and the instrumentation used to characterize the test conditions and model response. The arc plasma generator and support equipment are discussed in Section 2.1. The test nozzles are described in Section 2.2. The fume collection system is described in Section 2.3, and the instrumentation is presented in Section 2.4.

2.1 ARC PLASMA GENERATOR

The Aerotherm 1-megawatt constricted arc plasma generator (APG) is shown schematically in Figure 1a and physically in Figure 1b. This APG is a constant mass flow rate device with a flow rate controlled by throttling at the gas injection ports. The APG uses a segmented constrictor arc with a tungsten cathode and a water cooled copper anode to transfer energy to the primary test gas. This test gas is injected tangentially between the cathode and the first constrictor segment to provide a stable, high voltage operation. Additional gases to simulate propellant gases are injected downstream of the anode and mixed with the primary arc-heated gas in a plenum chamber. Thermochemical equilibrium is achieved in this plenum and the resulting simulation gases are expanded through a choked converging-diverging nozzle. The test section is the throat region of this nozzle.

The arc unit is water cooled with ambient temperature, high pressure deionized water. The APG input power is supplied by a 660 kw continuous rated, saturable core reactor, dc rectifier power supply. A maximum overload power level of 1.2 MW is achievable for 5 minutes. The power supply has 1,000, 2,000, or 4,000 volts open circuit voltage modes to match APG operating characteristics for various test gases, flow rates, and pressures. Arc starting is accomplished by imposing power supply open circuit voltages across the APG electrodes while an argon flow is maintained. Then a momentary RF discharge in the APG column provides an initial ionization path for the arc. Once the arc is started, test gases are immediately introduced as necessary to provide the required test gas composition.

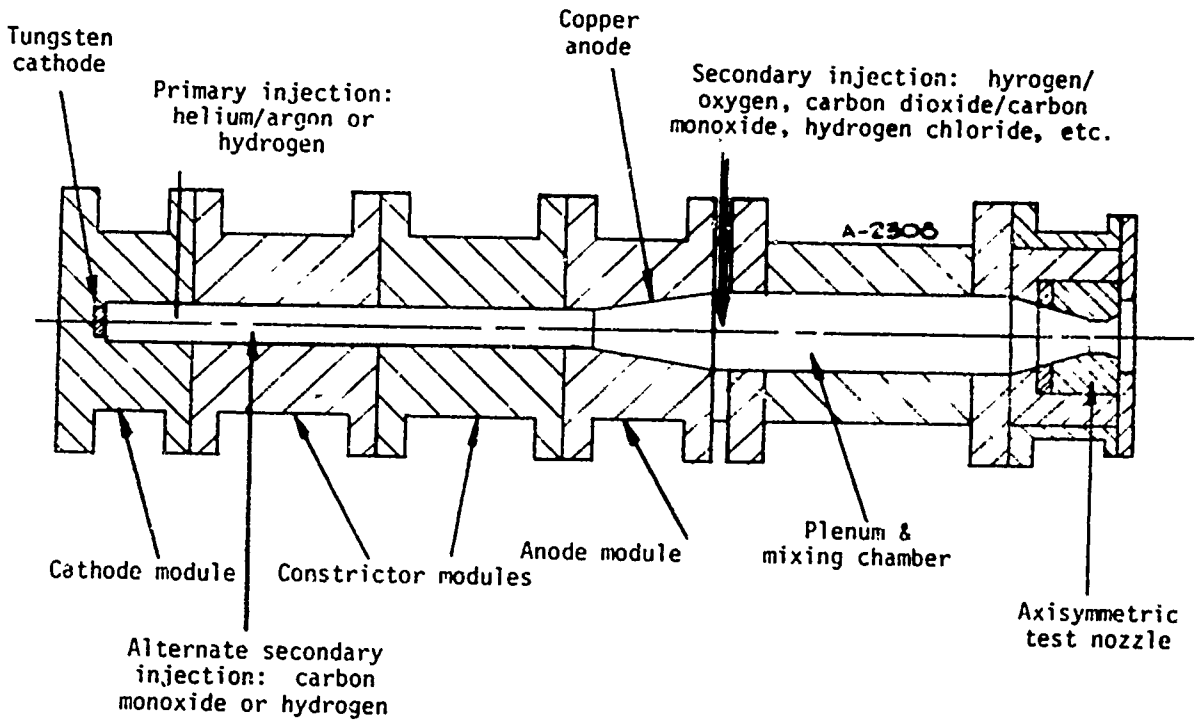

Figure 1a. Aerotherm 1-MW constrictor arc heater.

Reproduced from
best available copy.

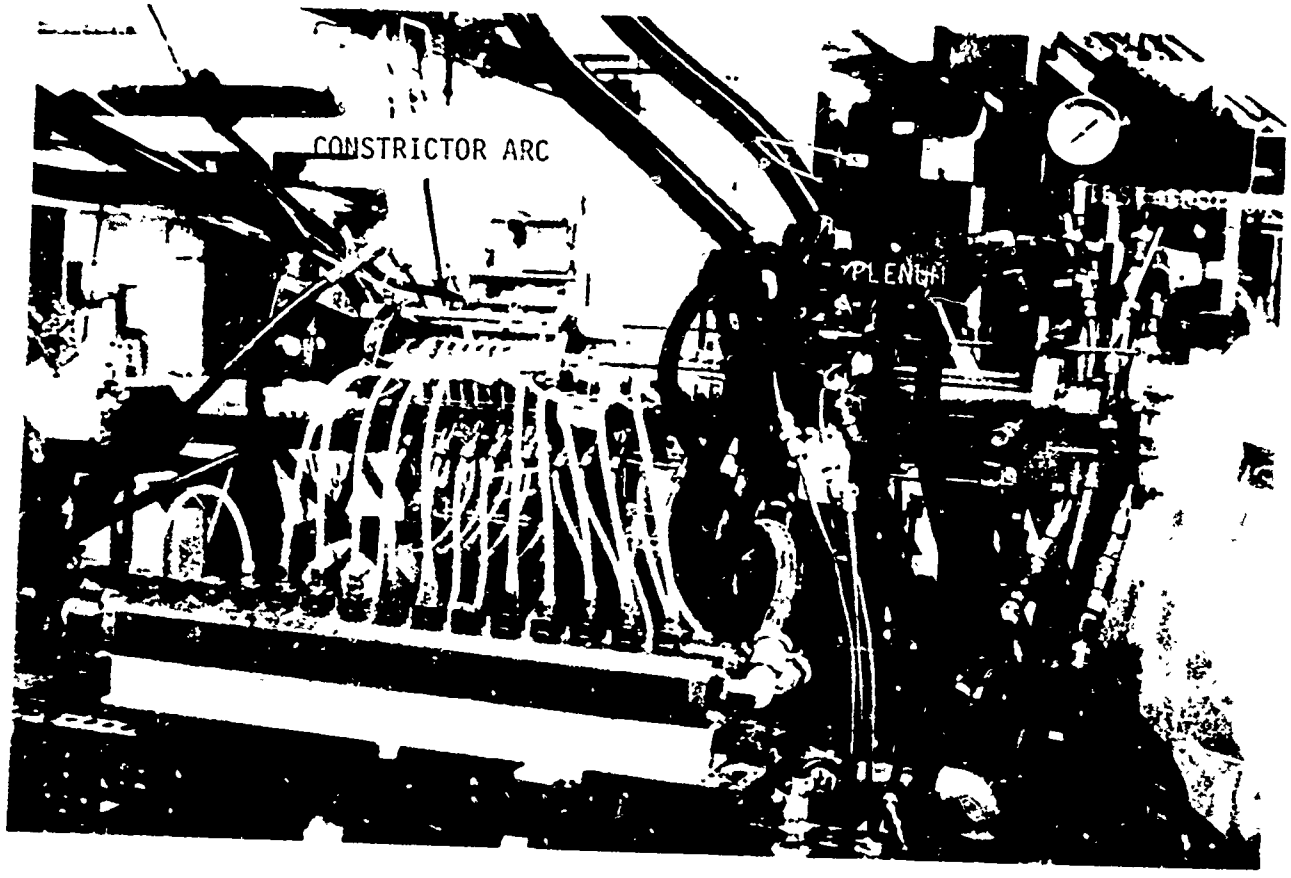

Figure 1b. Aerotherm 1-MW constrictor arc heater.

The arc unit exhibits very low contamination levels. Based on the results of Reference 2, total gas stream contamination should not exceed 200 parts per million (0.02 percent). The source of this contamination is the tungsten cathode and copper anode. A third potential source of contamination is the boron nitride insulators of the constrictor section; however, their contribution to the above figure is felt to be very small.

2.2 TEST NOZZLE CONFIGURATIONS

The nominal test configuration is an axisymmetric nozzle as shown in Figure 2. The test section inserts form the throat region of the nozzle. The PG washer immediately upstream of the test section insert insures a smooth transition into the insert and holds the boundary layer trip. This trip, a thin Grafoil disk, is employed to promote turbulent flow, and therefore high transfer coefficients, in the throat. The test section insert is retained by a crushable high temperature insulator. The test section could therefore expand thermally without imposing excessive compressive stresses. The test section insert configuration is shown in Figure 3. This is the nominal-dimension configuration; the details of the actual test insert depends on the particular requirements of the test material, e.g., backwall insulation in the throat region.

An appropriate ablation sample or a water cooled steady state calorimeter can be placed in the test section. The calorimeter and test sample both have the nominal interior dimensions shown in Figure 3 so that the test conditions during an ablation test can be inferred from a corresponding calorimeter test. The calorimeter installation is shown in Figure 4 and a view of the assembly is shown in Figure 5.

2.3 FUME COLLECTION SYSTEM

The APG for these tests is run on the atmospheric test stand with the test gases exiting directly into the test bay. A fume collection system is employed to collect, cool, clean, and exhaust the gases outside the test area. The system is shown schematically in Figure 6.

The first component of the system is the heat exchanger section. The high temperature of the test gases as they leave the APG requires a "cooldown" to less than 250°F before they enter the remainder of the system. This section is constructed of a high temperature alloy, Hastelloy Alloy C-276, and provides a set of spray nozzles which "quench" or cool the gases with a water spray. Also included in this section are two view ports to allow pyrometer viewing of the test section.

The gases are then ducted to the fume scrubber mounted outside the test bay. This scrubber is of the packed tower type and is designed to remove all toxic fumes (HCℓ, HF) from the gas stream before they are exhausted to the atmosphere. The scrubbing fluid is water used in the once-through mode.

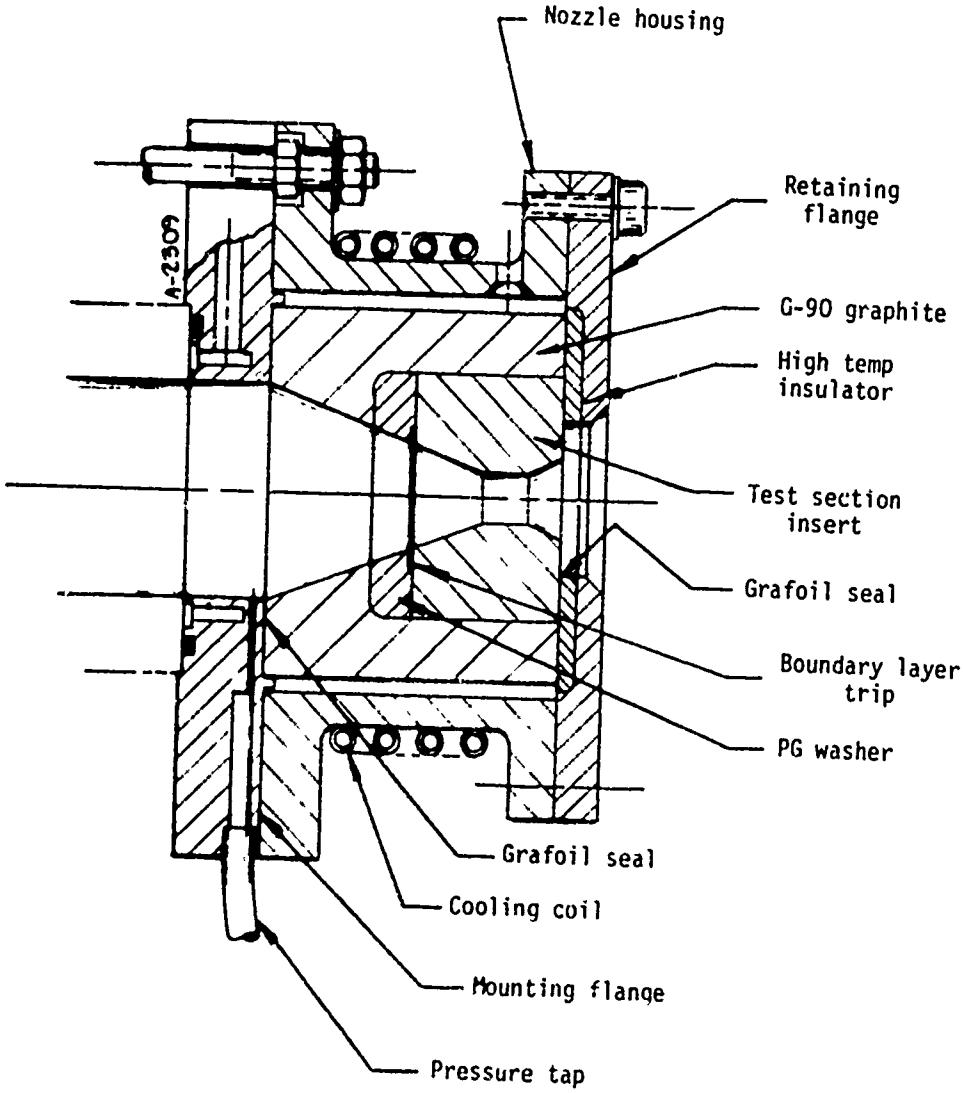

Figure 2. Axisymmetric nozzle assembly.

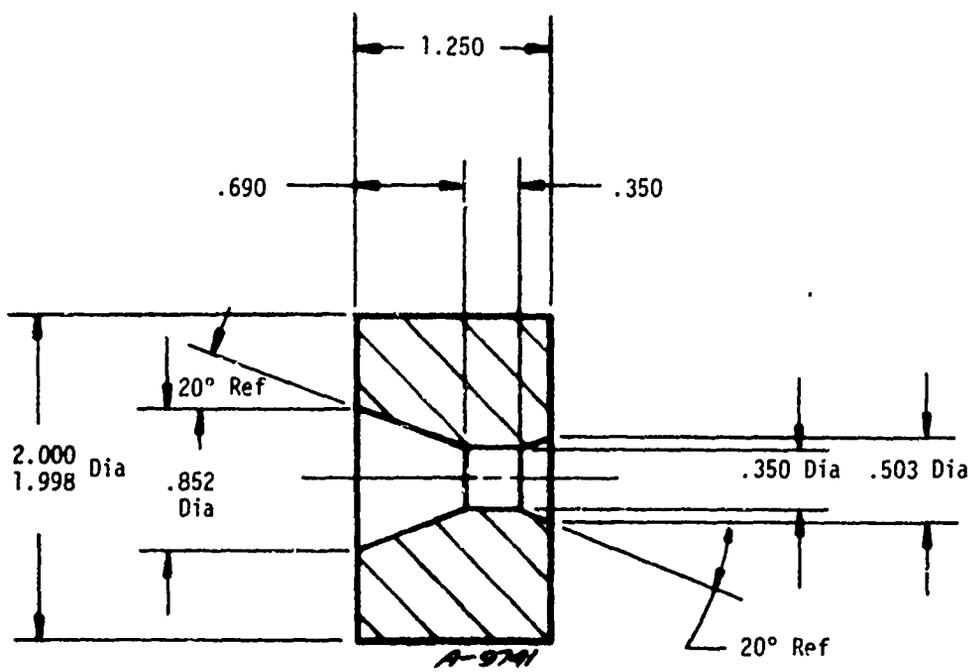

Figure 3. Nominal test section insert configuration.

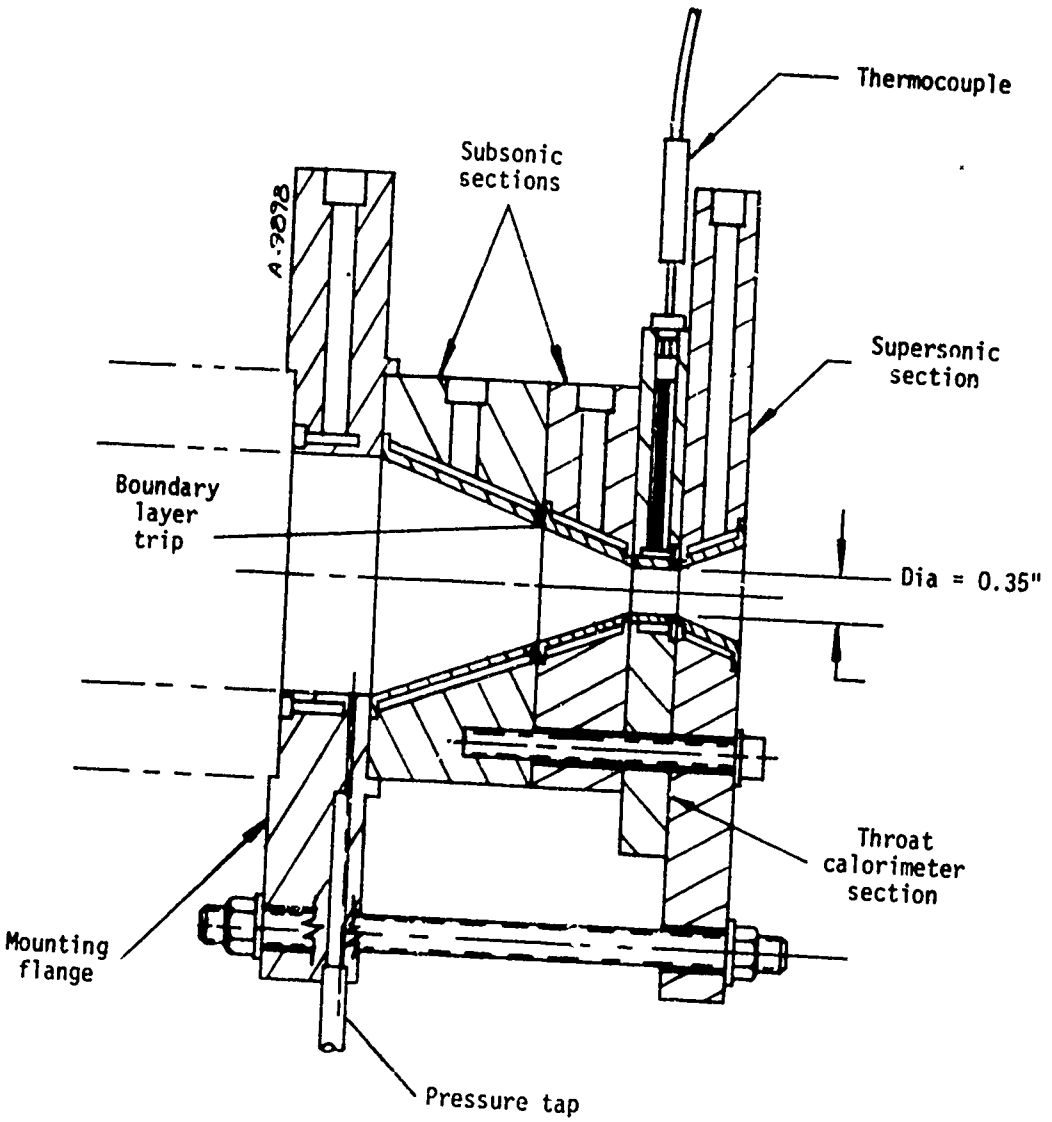

Figure 4. Calorimeter nozzle assembly.

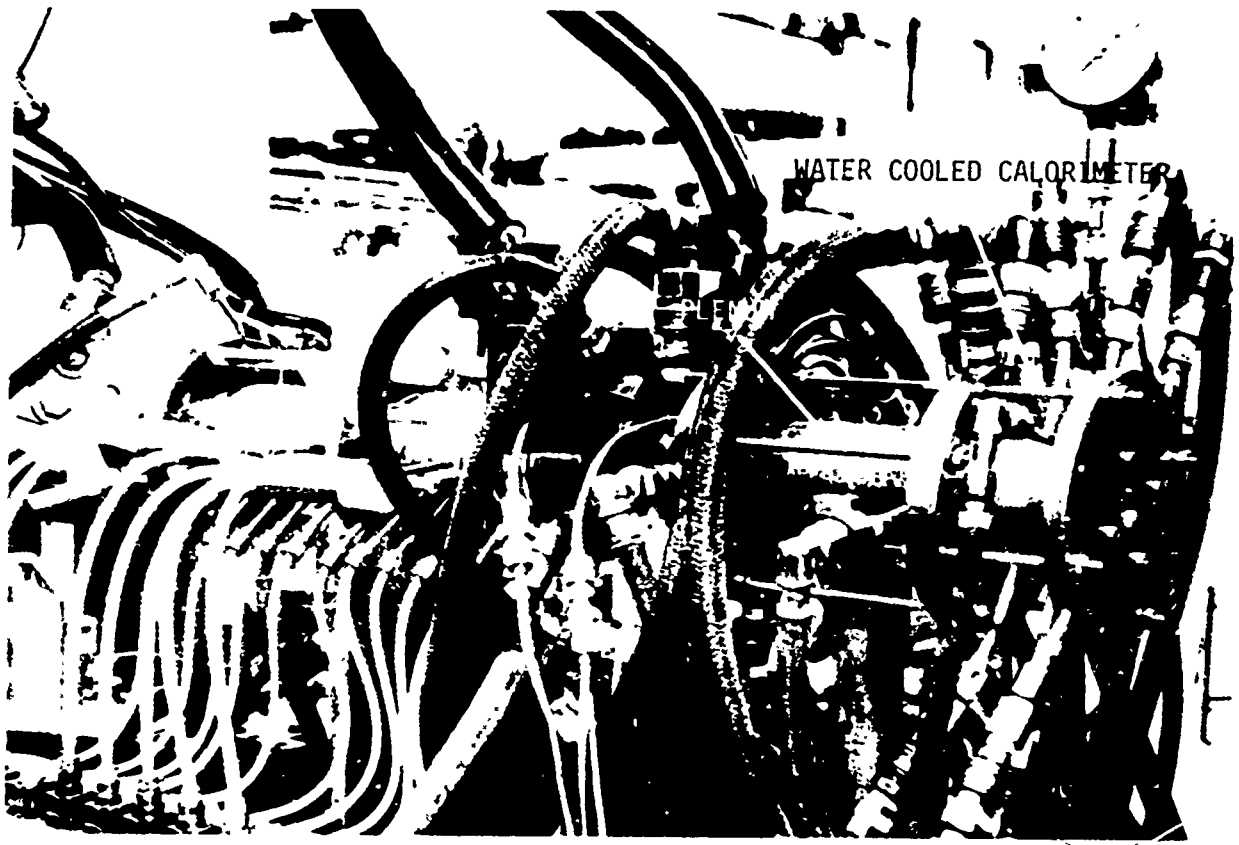

Figure 5. Axisymmetric test section, Calorimeter installed.

Reproduced from best available copy.

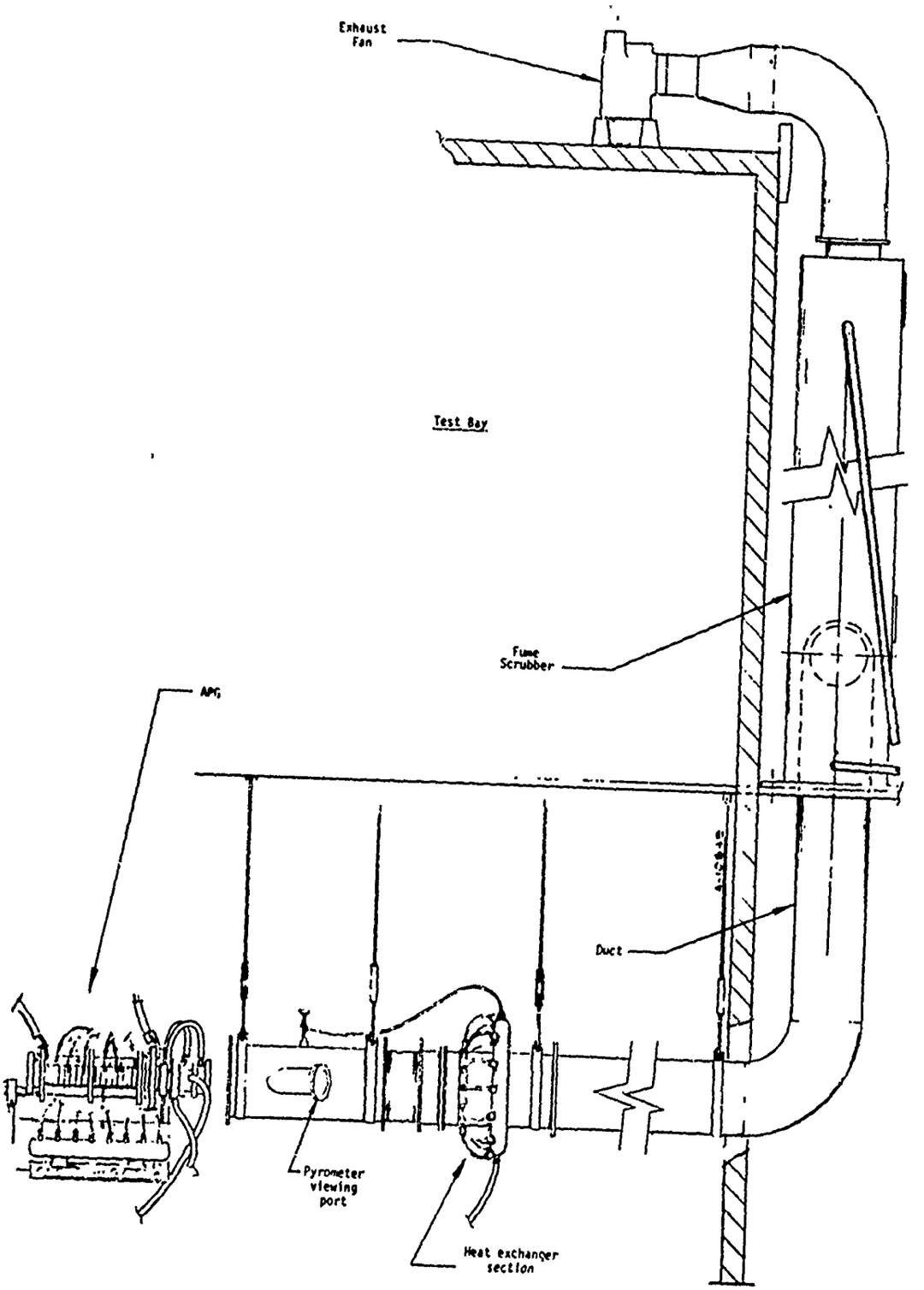

Figure 6. Fume collection system.

The final component of the system is the exhaust fan, mounted on the roof of the test bay. This provides the positive draft required to draw the gases through the heat exchanger section and the scrubber. The fan has been sized to provide a slightly negative pressure in the system when it is used in the blanked-off mode. This is necessary when hazardous or toxic test gases are used as it prevents the release of such gases into the test bay and insures personal safety.

Due to the corrosive nature of certain of the test gases (HCℓ or HF), the fan, scrubber and all ducting exclusive of the heat exchanger section are constructed of Rigedon 4837-AT-HF. This is a fire-retardant, fiberglass reinforced polyester plastic resistant to corrosive attack by both acids and alkali and, in addition, is provided with a special Dynel veil for protection against flouride attack.

2.4 INSTRUMENTATION

The measurements to characterize the test conditions and material response are

- Test Conditions
  - Gas Total Enthalpy
  - Chamber Pressure
  - Cold Wall Heat Flux
- Material Response
  - Surface Temperature History
  - Surface Recession
  - Qualitative Surface Condition

The gas total enthalpy is defined by an energy balance on the arc heater including the plenum chamber, i.e.,

$$h_o - h_{amb} = \Delta h_{arc} = \frac{\text{Power In-Cooling Water Losses}}{\text{Total Gas Flow Rate}}$$

$$= \frac{0.948 \times 10^{-3}\ EI - \dot{m}_c \Delta T_c}{\dot{m}_{gas}}$$

where h_{amb} is the enthalpy of the test gases at room temperature. Voltage E and current I are recorded continuously on a digital data recording system; measurements from panel meters are also taken as a check. The cooling water flow rate, $\dot{m}_c$, is measured continuously during each test with a sharp-edge orifice and differential pressure transducer and its temperature rise, ΔT_c, is measured continuously

with a differential thermopile. The total gas flow rate, $\dot{m}_{gas}$, is the sum of all gas flow rates delivered to the APG. All gas flow rates are measured with ASME sharp-edged orifices and differential pressure gauges, except hydrogen-chloride which is measured with a rotameter with a magnetic float follower.

The chamber pressure is measured continuously with strain gauge pressure transducers. The pressure taps are located at the downstream end of the plenum-mixing chamber (Figures 2 and 4). The chamber temperature is determined from the calculated net enthalpy addition due to arc heating, the measured chamber pressure, the test gas composition, and an ACE computer code computation of chamber conditions.

Cold wall heat flux is measured at the throat of the water cooled copper calibration nozzle with a steady state, water cooled calorimeter section. The coolant water temperature rise ΔT_c is measured with a single-pair copper-constantan differential thermopile, the output of which is recorded continuously. The calorimeter water flow, $\dot{m}_c$, is measured with a standard glass tube rotameter and the heat flux is then calculated from the equation

$$\dot{q}_{cw} = \frac{\dot{m}_c \Delta T_c}{A_c}$$

where A_c is the calorimeter heated area.

Surface temperature history is measured with an E^2 Thermodot TD-9CH optical pyrometer which is calibrated with a high temperature source. For each nozzle ablation test, this pyrometer, which has a sensing wavelength of 0.8 microns, views the nozzle throat at an angle of approximately 40° from the APG centerline. Output data is recorded both visually from the instrument meter and in digital form from the data acquisition system. In some tests, a second pyrometer is used as a check on the primary unit. This secondary unit is a Thermodot TD-9FH optical pyrometer similar to the primary instrument except calibrated in degrees Fahrenheit.

The test sample surface recession is obtained from pre- and post-test measurements of the throat diameter. Measurements are made at three axial stations in the throat region, namely, the entrance, center , and exit. In addition, at each station, the diameters are determined at two angular positions 90° apart. The measurement accuracy is approximately $\pm$0.0005 inch.

SECTION 3

TEST GASES AND TEST CONDITIONS

3.1 TEST GAS SELECTION CRITERIA

The selection of gases for APG testing is very important since ideally one would like to minimize the extent to which experimental results must be extrapolated in order to predict actual conditions. Several questions must therefore be addressed in selecting appropriate gases.

1. What rocket motor environments are anticipated?
2. What are the important surface reactions?
3. What information is required in the prediction procedure?
4. How sensitive is the kinetic response to predicted variables such as the heat or mass transfer coefficient?
5. What are the operating limitations of the APG?

Test gases must be defined for two different kinds of test. On the one hand a comprehensive set of gas mixtures must be defined to allow a full kinetic characterization of the test material. On the other hand a gas mixture or a set of gas mixtures must be defined for experimental screening or ranking of materials which are similar to those which have received the full characterization treatment. Although it is likely but not necessary, the screening gases and their test conditions will be a subset of the full characterization test matrix.

3.1.1 Rocket Motor Environments

Rocket motor environments will be based on three advanced MX propellants, namely,

- XLDB
- HTPB
- PEG/FEFD

Representative elemental compositions and flame temperatures are given in Table 1. For the purpose of studying surface kinetics only the elemental composition of the propellant gas need be considered. The solid Al_2O_3 does not enter into the

TABLE 1. REPRESENTATIVE COMPOSITION AND FLAME TEMPERATURE OF ADVANCED MX PROPELLANTS

Propellant	XLDB	HTPB	PEG/FEFO
Flame Temperatures (°K)	3880	3690	3787
(°F)	6524	6182	6360
Mass Fraction			
H	2.5	4.0	2.6
C	13.5	8.4	12.5
N	24.0	9.0	23.0
O	39.5	40.0	37.9
F	—	—	1.5
Al	18.5	17.6	18.5
Cl	2.0	21.0	4.0

TABLE 2. PROPELLANT GAS COMPOSITION (Al_2O_3 REMOVED)

Propellant	XLDB	HTPB	PEG/FEFO
Mass Fraction			
H	3.8	6.1	4.0
C	20.8	12.7	19.2
N	36.9	13.6	35.4
O	35.5	35.2	32.9
F	—	—	2.3
Cl	3.0	32.4	6.2

surface kinetics problem although it probably contributes to surface erosion rates. Table 2 gives representative compositions of the propellant gases with all the Aℓ and an appropriate amount of oxygen removed as $Aℓ_2O_3$. The ACE/GASKET program was used to determine the concentration of gas species which would exist at the carbon surface for three conditions: (1) surface equilibrium, (2) very small surface ablation, and (3) a nonreacting surface at typical surface temperatures (2200°K to 3300°K). Those species with significant concentrations would then be candidates for reactants and/or poisons. A typical distribution of surface species as a function of temperature for an HTPB propellant is shown in Figure 7. This solution represents the kinetically controlled ablation of edge oriented pyrolytic graphite at a throat pressure at 39.4 atm from the ACE/GASKET calculations. Those species considered as possibly significant reactants (molar concentrations greater than 0.1 percent) are:

- CO
- H_2O
- H_2
- N_2
- CO_2
- HCℓ
- HF (HF not a specie for the HTPB solution)

It should be noted that other species, such as Cℓ and H, appear in representative amount and may also be important. Still other species, such as O and OH, though present only in small quantities may have very fast reaction rates. These latter species vanish very rapidly as ablation rate increases so that they would probably increase rates only a slight amount before they are depleted. Atomic hydrogen has been shown, at least on one case*, to react slower than H_2 and since the concentrations of H_2 are an order of magnitude greater than that of H, ablation due to the latter will probably be insignificant. Cℓ, a halogen, is a potential poison, however, there is no firm evidence for this behavior. Thus, the species of interest are those previously listed.

3.1.2 Important Surface Reactions

The most probable surface reactions can be identified by considering the available species, the possible reactions with carbon, and the equilibrium constant for each reaction. (The equilibrium rate serves as an upper limit to the surface kinetic rate.) Of the reactions considered, only the following have sufficiently large equilibrium constants in the temperature range of interest:

---

*Personal Communication. Professor D. Rosner, Yale University.

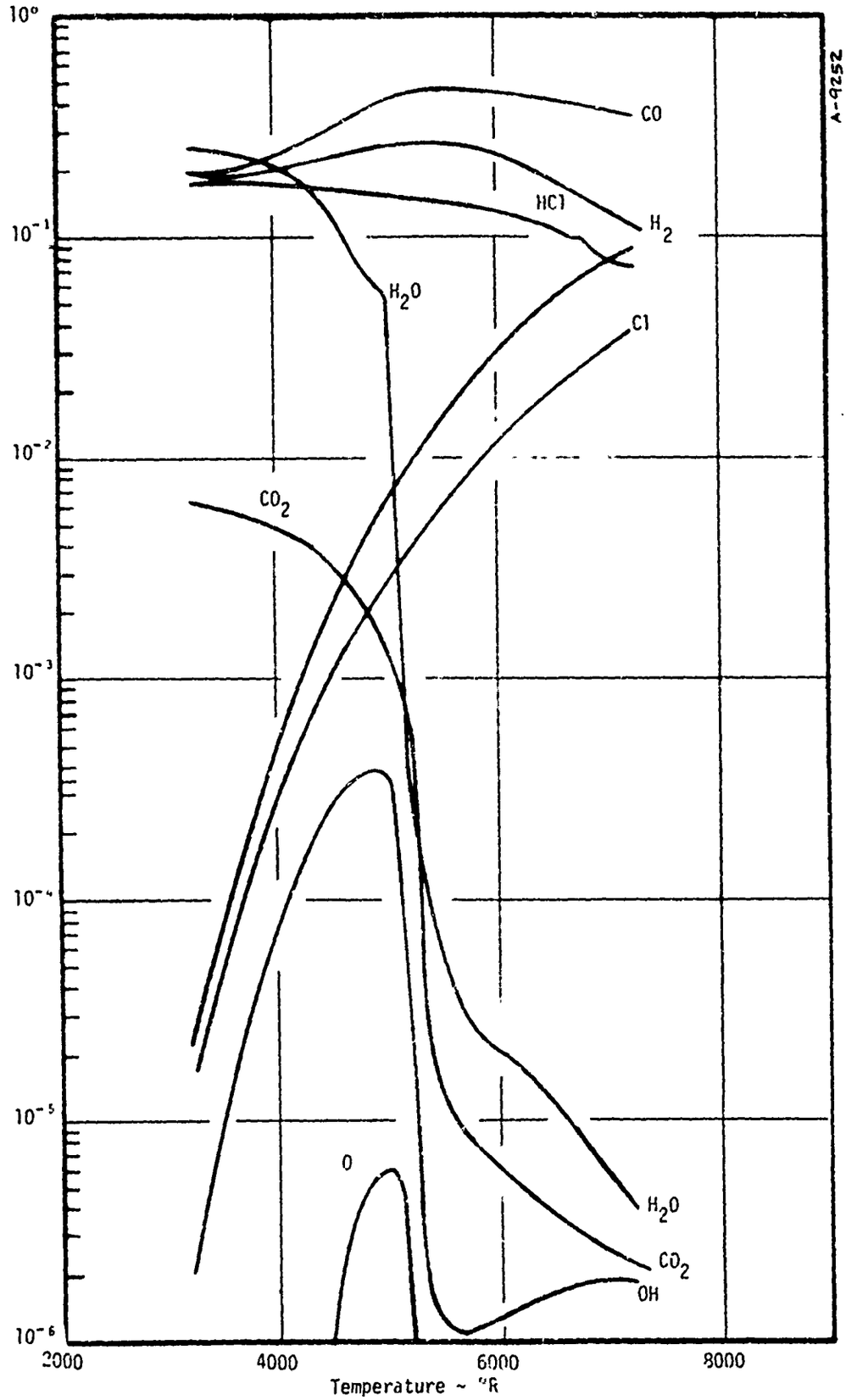

Figure 7. Typical surface gas composition at throat for C-Plane PG

$$C^* + H_2O \rightarrow CO + H_2$$

$$C^* + CO_2 \rightarrow 2CO$$

$$2C^* + H_2 \rightarrow C_2H_2 \ ^{\dagger}$$

The reactions of carbon with CO, N_2, HCℓ, and HF are not considered significant since the equilibrium formation rates are too small. However, they may have innibitor properties.

The mechanism of poisoning, or inhibition of surface reactions, is basically one of active site competition. That is, a poison specie may occupy an active lattice site and thus prevent a reactant from occupying that site. Of the seven species listed as possible poisons, only N_2 will not be considered because it appears to be inert as far as surface kinetics are concerned.[§] Although H_2O and CO_2 readily react with the carbon surface they are, nevertheless, occupying lattice sites and thus, in that sense, are poisons for each other.

3.1.3 Required Information for Predictions

The singular purpose of this experimental program is to provide empirical data to be used in an analytical procedure for predicting rocket nozzle thermal performance. The expression desired in Reference 1 for kinetic ablation rates of graphitic materials is

$$\dot{m}_c = MC \cdot \left\{ \frac{\left(p_{H_2O} + A' p_{CO_2} \right)}{(D_1 \times D_2)} + \frac{MCH \times p_{H_2}}{D_3} \right\} \qquad (1)$$

where

$$D_1 = \left[1 + (Ap)_{H_2O} + (Ap)_{CO_2} + (Ap)_{CO} + (Ap)_{H_2} \right] \qquad (2)$$

$$D_2 = \left[1 + (Ap)_{HC\ell} \right]$$

$$D_3 = \left[1 + (A''p)_{H_2O} + (A''p)_{CO_2} + (A''p)_{CO} + (A''p)_{H_2} \right]$$

[†]Although C_2H_2 does not appear in the list of gas species, the reactions should not be ruled out. Hydrogen is present in large concentrations (approximately 25 percent by mole) and the C_2H_2 coming off the surface may be eliminated by gas phase reactions.

[§]Kinetic rate data in Reference 1 substantiates the inert behavior of N_2.

$$MCH = B_2/B_1 e^{-(E_2-E_1)/RT_w}$$

$$\equiv B_e^{-E'/RT_w}$$

The A, A', A", B, and E coefficients are the terms that must be determined from experimental data. Since temperature and a set of chemical species are involved, the experiental data must vary these variables over a sufficient range so as to allow the accurate definition in a data correlation procedure. As noted, the APG provides wide latitude on gas composition over a limited temperature range. By simultaneously including rocket motor data, the correlation procedure can be extended over a relevant temperature range. This is done with the current data analysis scheme, however, for the present, only the APG data is of interest.

The term MC is the correlation parameter and is presumed to be a function of temperature only. For any given test it is then necessary to define $\dot{m}_c$, T_w, and p_i and for any given set of data, the correlation procedure must determine the coefficients A, A', A", B, and E such that in an MC versus T_w (or $1/T_w$) plane, the data has a minimum scatter. Experimentally, it is not possible without great agony to measure p_i in the vicinity of the hot ablating wall. In fact, it is not even necessary if $\dot{m}_c$ and T_w are measured and the elemental composition of the test gas is known. Since, at the test pressures and temperatures, the gases are probably in thermochemical equilibrium (homogeneously but not necessarily heterogeneously) the species composition and, hence, p_i can be calculated from an open system thermochemical computation using $\dot{m}_c$ and T_w.

Implicit in the thermochemical computation is a knowledge of the mass transfer coefficient ($\rho_e u_e C_m$). In an APG test this can be determined by calibration with appropriate heat transfer measurements; however, for rocket motors this can only be determined by analysis. Thus, an APG test measures all necessary variables (i.e., T_w, $\dot{m}_c$, and $\rho_e u_e C_m$) whereas a motor firing yields only total recession; T_w and $\rho_e u_e C_m$ must be determined or estimated by other means.

For the measured results to be relevant in an analytic procedure, the test gases and test conditions must be selected with care. This selection must be based on the above discussion on important gas species. But, in addition, the sensitivity of the gases on predicted results and APG limitations must also be considered. These considerations are discussed below.

3.1.4 Sensitivity of Kinetic Response

Since gasket and ACE are the only computer codes that are currently in use by manufacturers in the rocket community, the main concern here is to determine for a given kinetic model, the sensitivity of predicted results to input parameters. The

Aerojet Solid Propulsion Company MX nozzle was selected as the baseline configuration, and each parameter was studied to determine its influence on the surface thermochemistry solution. The parameters that were considered are: the thermodynamic state at the boundary layer edge; the mass transfer coefficient; and the kinetic constants at the surface reactions.

As a result of the sensitivity study, it was found that the sensitivity to the input thermodynamic state at the boundary layer edge is negligibly small. Sensitivity to the input of the mass transfer coefficient however, is dependent upon the magnitude of the kinetic constants used in the Arrhenius type expression. For the baseline case, at the location of the nozzle throat, the kinetic regimes of the following materials were determined as:

- Layer P.G. Temperature < 5900°R
- Edge P.G. Temperature < 4700°R
- Bulk graphite Temperature < 3600°R

At temperature below these thresnold temperature, it was found that the mass transfer coefficient had no significant role in the surface chemistry solution. Conversely, at temperature above the threshold temperature, the sensitivity to the input value of the mass transfer coefficient increased monotonically with temperature as the chemical reactions shifted from kinetic limiting to diffusive limiting.

Qualitative Description of Surface Thermochemistry

The surface thermochemical process can be best described by the following equation

$$J_i = \frac{C_{i_e}}{\frac{1}{\beta_i} + \frac{1}{k_i}} \quad (3)$$

where J_i is the diffusion rate of the reactant i, C_{i_e} is the reactant concentration at the boundary layer edge, β_i is the mass transfer coefficient, and k_i is the kinetic constant. Note that Equation (3) only assumes a simple first order reaction and no inhibiting effect is considered. To account for complex kinetics, further modifications are required. The functional form of Equation (3) introduces a very useful interpretation when compared to electric network theory. By analogy, Ci_e can be considered as the driving potential, the reciprocals of the mass transfer coefficient and the kinetic constant as the surface resistance, and the flow of the

*Reference 3

reactant as the current. It is interesting to note that when $k_i \gg \beta_i$, the rate of the overall process is then completely determined by the diffusion rate. Conversely, when $k_i \ll \beta_i$ the rate of the overall process is completely determined by the actual kinetics of the surface reaction. The former limiting regime is called the diffusion regime, the latter is called the kinetic regime, and the intermediate regime is called the transition regime.

In the sensitivity analysis, the effect of the following parameters was assessed:

- One-dimensional flow versus two-dimensional flow (shows effect of the edge thermodynamic state)
- Equilibrium flow versus frozen flow
- Mass transfer coefficient for ab-plane PG, C-plane PG, and bulk graphite (shows the kinetic regimes of the three materials)
- Mass transfer coefficient versus erosion rate (wall temperature at 6000°R)

The baseline case was a typical MX upper stage nozzle contour with a PEG/FEFO propellant expanded from typical chamber conditions to the throat (sonic point). The option of equal diffusion with a unity Lewis number was chosen in order to simplify the analysis, however, the effect of unequal diffision, Lewis No. 1 will be addressed later.

Table 3 shows the sonic point thermodynamic states at the boundary layer edge as calculated for 1-D equilibrium flow, 2-D equilibrium flow, and 1-D frozen core flow conditions. It was found that the 1-D frozen flow predicted a higher pressure and higher concentrations of the three major reactants (steam, carbon dioxide, hydrogen).

TABLE 3. MX BASELINE – PEG/FEFO PROPELLANT THROAT THERMODYNAMICS CONDITIONS AT BOUNDARY LAYER EDGE

Type of Flow Field	P_e (atm)	T_r (°R)	Reactant Concentration (lb-mole/ft^3)		
			CO_2	H_2	H_2O
1-D Equil.	57.72	6467	8.93×10^{-5}	3.26×10^{-3}	5.89×10^{-4}
1-D Frozen	63.43	6343	10.51×10^{-5}	3.44×10^{-3}	6.92×10^{-4}
2-D Equil.	47.74	6378	7.31×10^{-5}	2.70×10^{-3}	4.80×10^{-4}

Based on Equation (3) and the reactant compositions shown in Table 3, 1-D flow assumptions should result in higher erosion rates. However, as shown in Figure 8 for PG washers, there is no discernable dependence of the mass loss versus temperature relationship on boundary layer edge state* for temperatures below 6500°R and only small differences are observed for higher temperatures. These results, though unexpected, are not surprising since the derivation of Equation (3) does not account for inhibiting effects. In the case considered here, reactants are competing for active sites at the surface. Hence a species which serves as a reactant for a particular surface reactant, may very well be an inhibitor to the other reactions which simultaneously take place at the surface. This competing phenomenon may be the reason why no appreciable influence is observed.

Figure 8 through 10 show that for each graphitic material there is a regime where the ablation rate is insensitive to the magnitude of the heat transfer coefficient. This regime as described in the above section is called kinetic regime. As can be seen in these figures, the kinetically limited regimes are as follows:

- Layer P.G. Temperature < 6500°R
- Edge P.G. Temperature < 4800°R
- Bulk graphite Temperature < 3600°R

It is apparent that below the threshold temperatures, the surface thermochemistry is independent of the mass transfer coefficient. However, at temperature above the threshold temperatures, the dependence increases as temperature increases. At a sufficiently high temperature the surface reaction reaches equilibrium, and the ablation rate is controlled by diffusion which has a linear dependency on the mass transfer coefficient. Surface characteristics are then no longer important and all carbons will ablate at the same rate. Figure 11 presents the results which are predicted by surface equilibrium considerations.

Figure 12 presents a more explicit picture of how the erosion rate depends on the mass transfer coefficient. The dotted line is the surface equilibrium predictions which show that the erosion rate is a linear function of the mass transfer coefficient. As expected, based on Equation (3), when $\rho_e u_e C_m \to \infty$, the erosion rate becomes independent of the mass transfer coefficient. Though this is not as evident in the bulk graphite solution as in the layer and edge P.G. solutions.

The unequal diffusion process accounts for the molecular weight differences between species upon diffusion from the boundary layer edge to the surface and vice versa. The lighter molecules diffuse faster than the heavier molecules since their

*Note that this statements applys only for edge states at the nozzle throat as predicted by different gas expansion assumptions starting with the same chamber conditions.

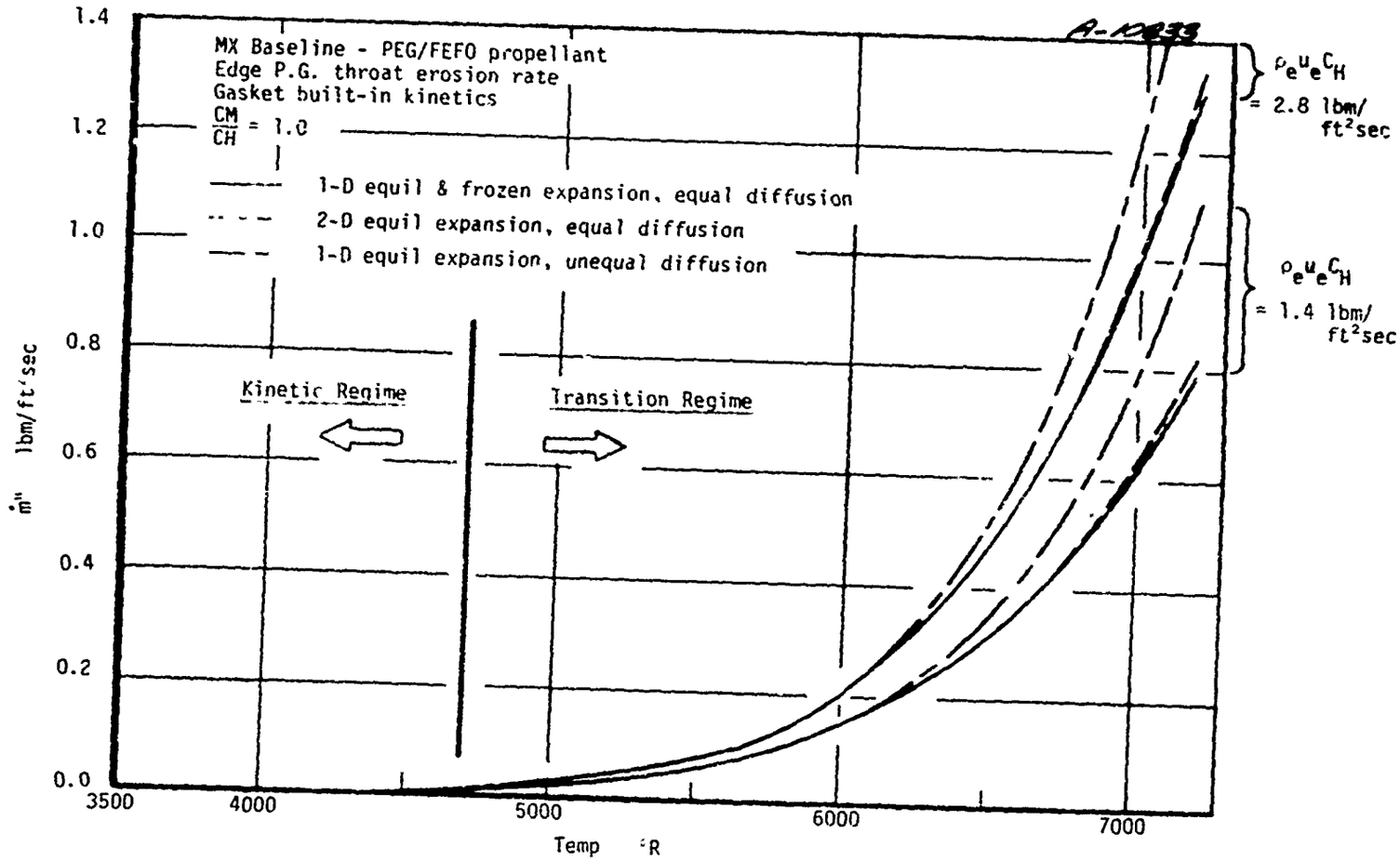

Figure 8. Effect of boundary layer edge on carbon consumption rates.

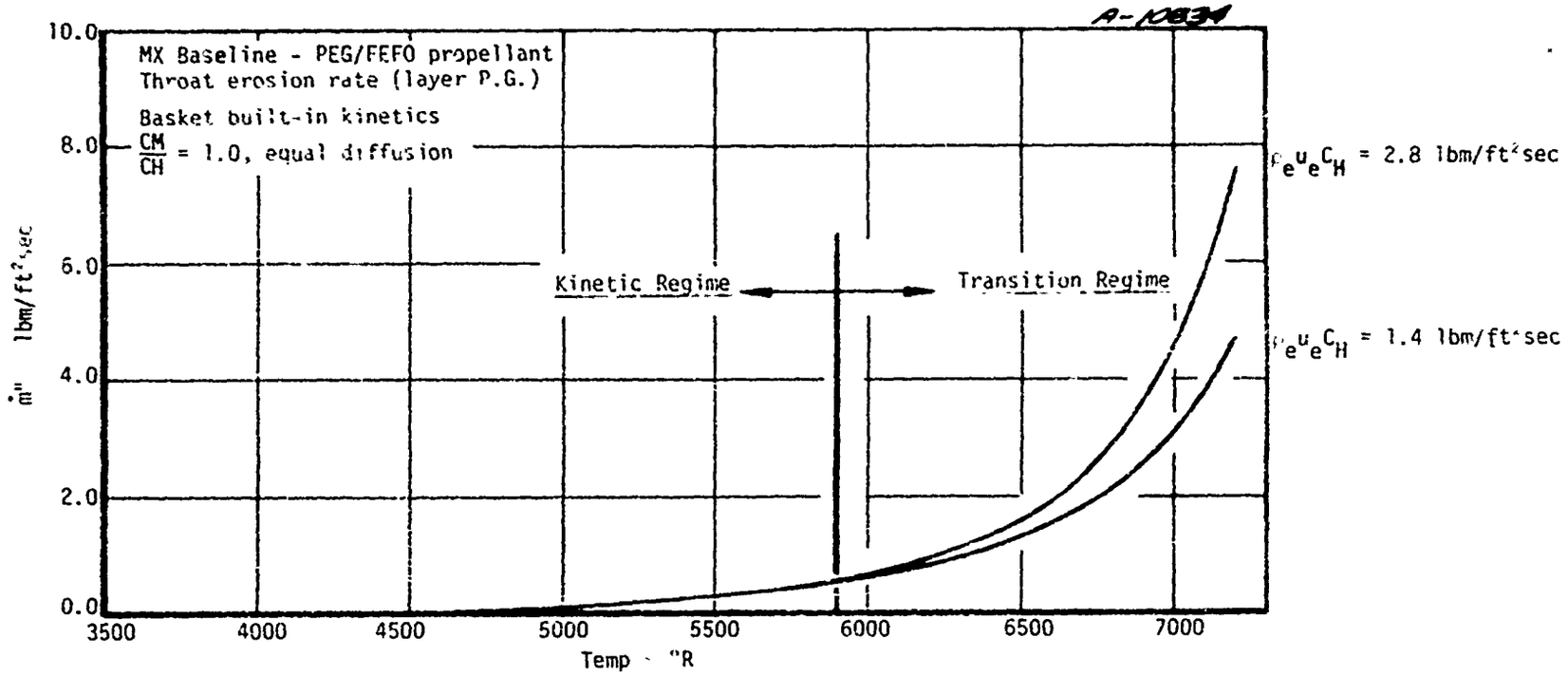

Figure 9. Delineation of kinetic and transition regimes for A-B Plane PG.

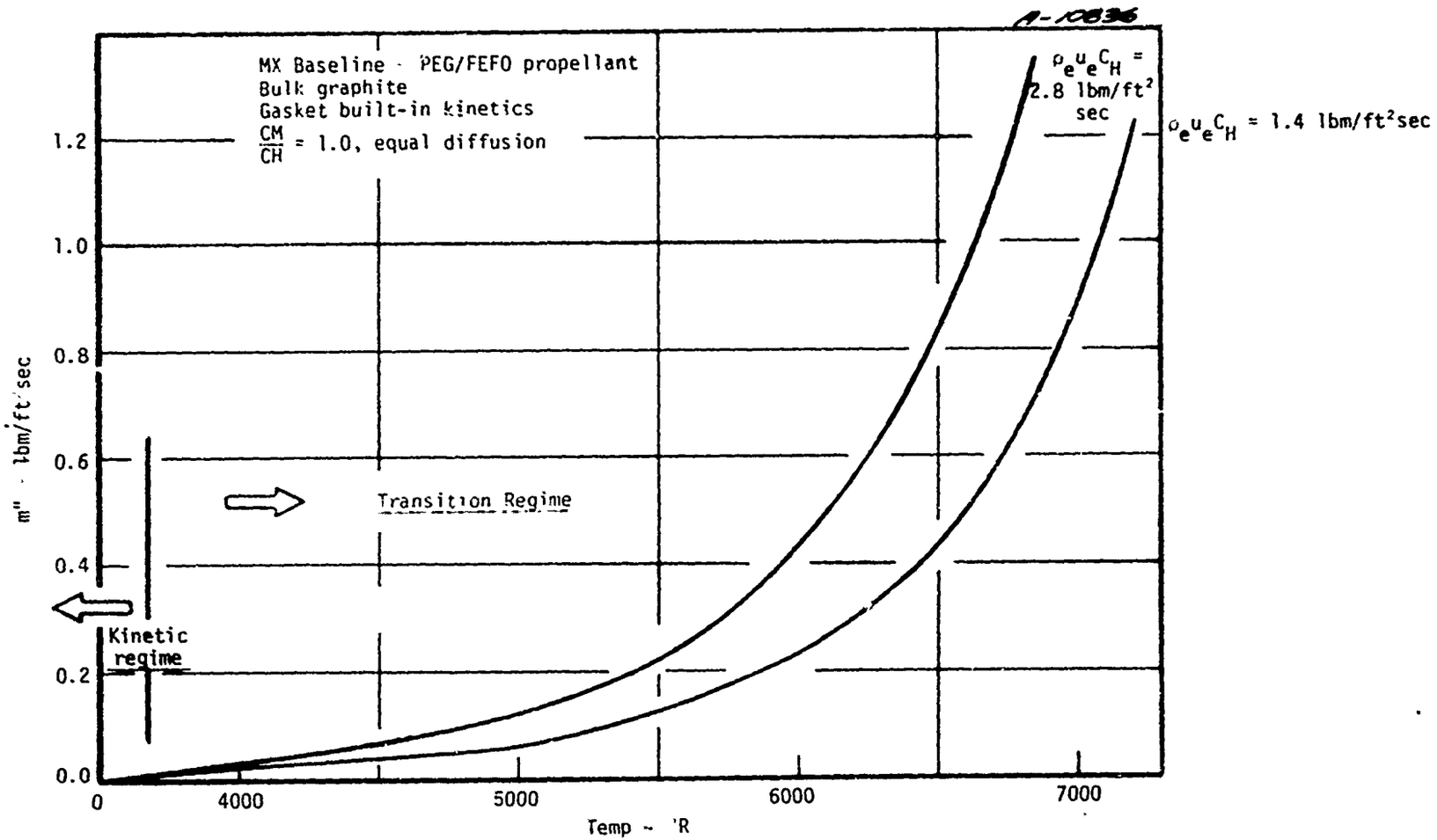

Figure 10. Delineation of kinetic and transition regimes for bulk graphite.

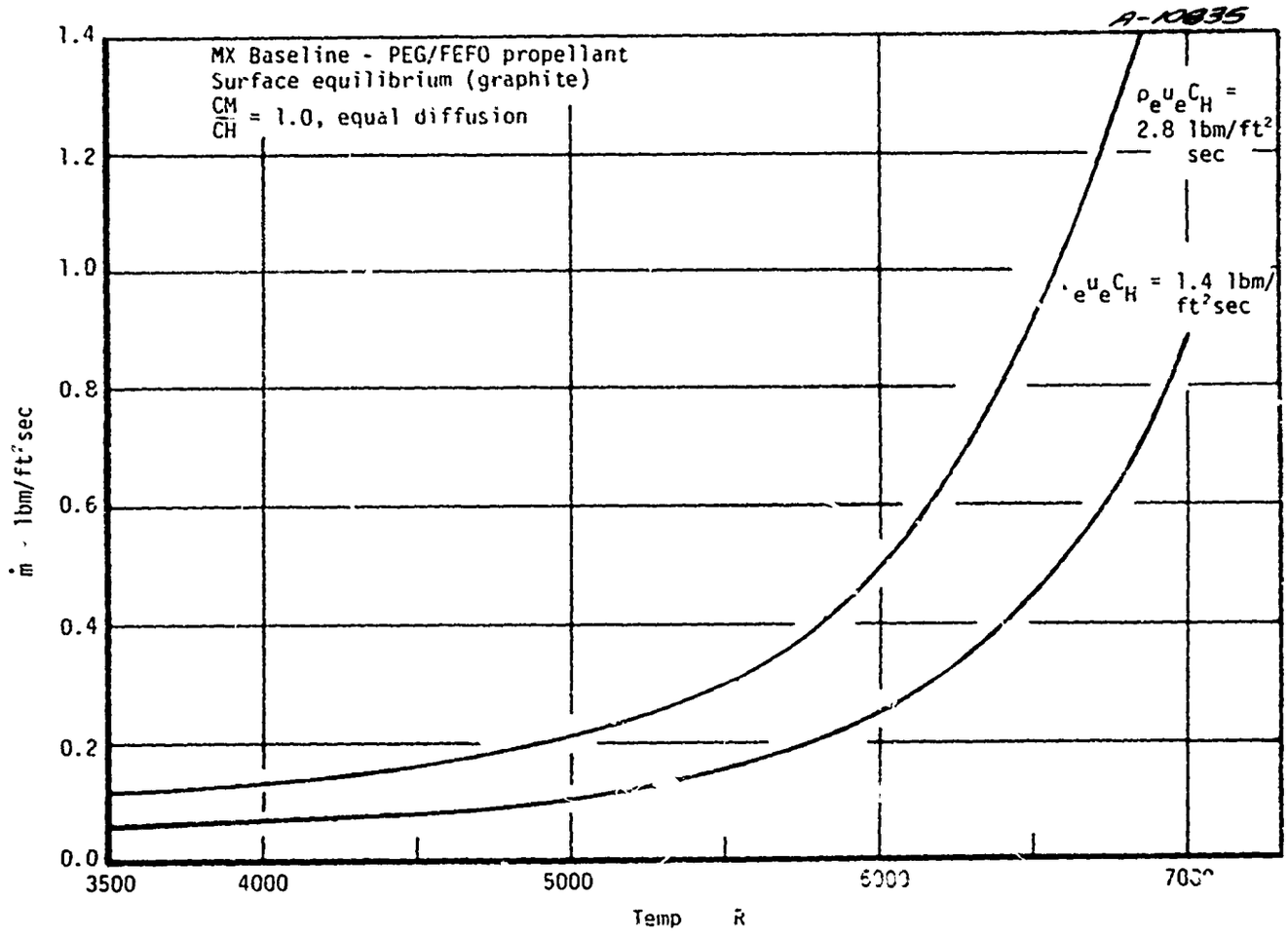

Figure 11. Equilibrium graphite consumption rates.

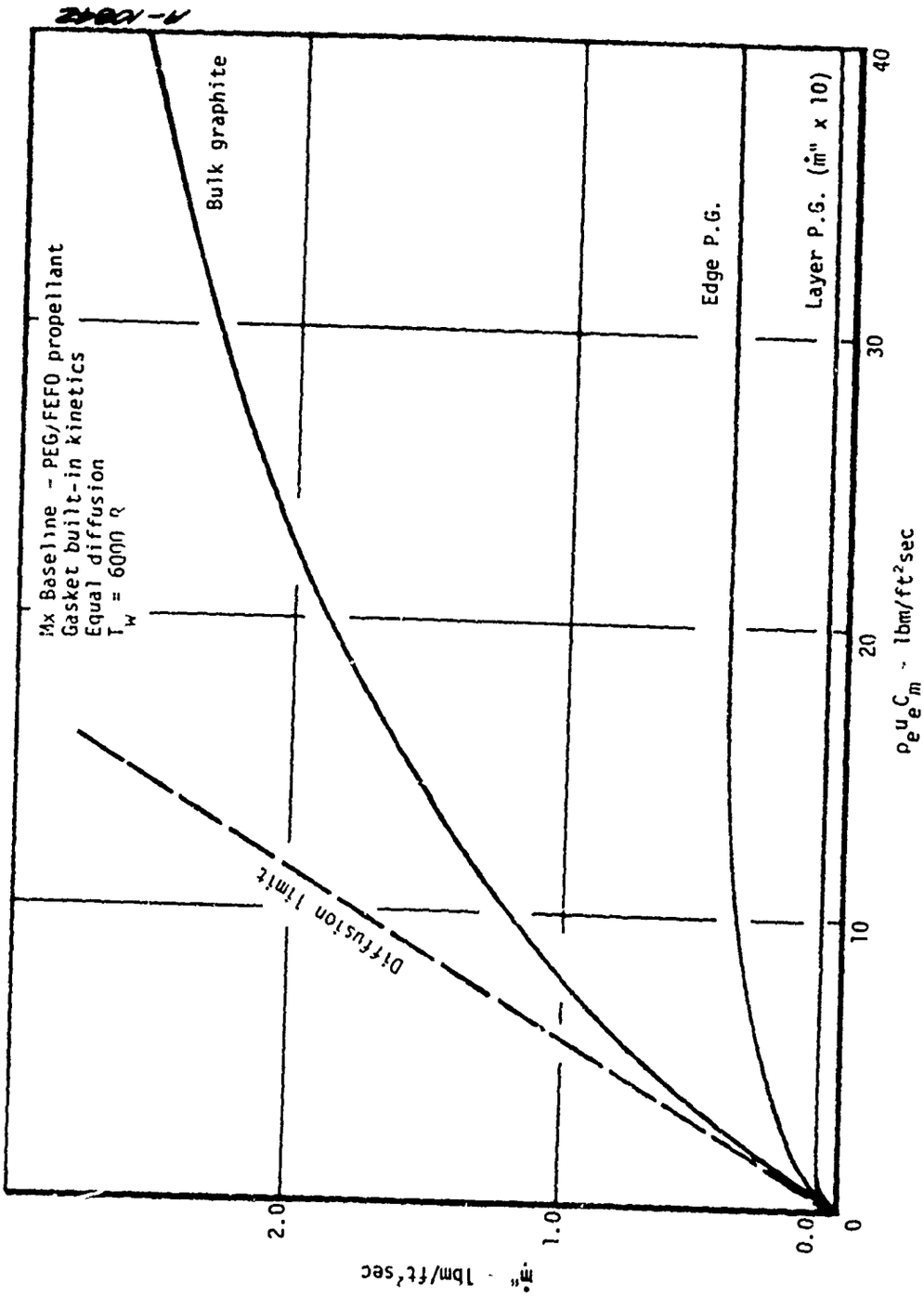

Figure 12. Effect of mass transfer coefficient on graphite consumption rates.

mean free paths are larger and hence allow them to travel farther before colliding with other molecules. Therefore, in a hydrogen rich environment, which is often the case for propellant combustion gases, the equal diffusion assumption will underpredict the diffusion rate. For layer P.G., due to the slow surface reactions, the diffusion process does not affect the erosion rate at all. Figure 12 shows that the erosion rate is constant at a typical wall temperature of 6000°R over a wide range of $\rho_e u_e C_m$. With edge P.G. which has a stronger dependency on $\rho_e u_e C_m$, variations on the erosion rate prediction were found (see Figure 8) at temperature above 6000°R. The determination of the kinetic regime, however, is not affected. Obviously, the bulk graphite predictions are going to be affected, as it also has a strong dependency on $\rho_e u_e C_m$.

The Lewis number is the nondimensional group which characterizes the relationship between the energy and mass transports. The correlation frequently employed (Reference 4) is

$$\frac{C_M}{C_H} = Le^{2/3} \tag{4}$$

Generally, $Le \neq 1$, and hence it has an effect on the erosion rate predictions. Again, the predictions of layer P.G. are unlikely to be affected. Edge P.G. and bulk graphite will undoubtedly be affected as shown in Figure 8. The erosion rates are expected to decrease if $Le < 1$, and vice versa.

From the above discussion, one can conclude that both data analysis and ablation predictions require a careful evaluation of the transfer coefficient. In addition, when large quantities of hydrogen are in the gas, unequal diffusion should be included in all calculations.

3.1.5 Arc Plasma Generator Limitations

The design and operation of the arc plasma generator imposes restrictions on the choice and use of certain test gases. There are two basic areas of concern; first, the effect of a particular gas on the vital components of the APG (cathode, anode, constrictor segments, etc.) and second, the stability of the arc when operating with a particular gas or combination of gases. The situation is further complicated by the desire to produce a test gas at as high a temperature as possible. This generally requires arc heating of the largest possible portion of the total test gas flow to the maximum temperature achievable, i.e., maximum energy input, while minimizing the energy losses to the cooled walls of the APG.

With the design of the APG currently being used, it is necessary to avoid injecting any oxidizing species into the arc heater as the primary gas. This is due

to the tungsten material used in the cathode, which when rapidly removed through oxidation processes can both limit APG run times to the order of seconds and cause catastrophic failure of the arc heater. The normal solution employed is the injection of such gases several constrictor duct diameters downstream of the cathode. This has been highly successful when the required test gas is simulated air, using individually injected nitrogen and oxygen. However, in the case of propellant simulation, there is an additional problem. The reactive nature of the base species, hydrogen, which for reasons of arc efficiency and maximum power input is the arc heated gas, requires the injection of oxidizing species downstream of the arc heater portion of the APG, in the plenum section (see Figure 1a). This is primarily due to the combustion induced turbulence which adversely affects the stability of the arc, resulting in failure of the constrictor segments. Therefore, the primary or arc-heated gases must be either inert or nonoxidizing, the remainder of the test gases required to make up the propellant simulation are injected in the plenum section. This results in lower overall APG efficiences due to the portion of the test gas which is not directly arc heated and the losses to the plenum section from both the arc heated primary gases and the exothermic reactions which take place in the plenum. The net effect is lower test gas temperature and hence lower test sample surface temperature.

The "normal" APG limits of pressure, current and power input must also be considered. These, in general, are less severe than those discussed above and typically can be accommodated through arc heater and power supply configuration changes. It should be noted that this is especially true with hydrogen, which is very sensitive to the gas injection configuration and arc heater constrictor length. The penalty for use of an improper configuration is usually very unstable arc operation.

3.1.6 Potential Test Gases

As described in Section 3.1.2, the potentially important reactants are H_2, H_2O, and CO_2, typically in decreasing order of mole fractions (see Table 3). In an APG, various concentrations of these gases can be mixed and reacted to form the test stream. By judicious selection various reactants and poisons could be isolated in a systematic manner so that appropriate reaction rate constants could be determined. some kinetically appealing test gases are shown in Table 4. These gases are separated into three groups, reactions which include H_2, H_2O, CO_2, and CO, reactions with these gases and HCℓ, and reactions with HF in lieu of HCℓ. The surface reaction designations are shown in Table 5. The number of test gases to be used in a material characterization test matrix would be selected as a subset of the gases tested in Table 4. This selection will be based upon a trade-off between the degree

TABLE 4. POTENTIAL APG MATERIAL CHARACTERIZATION TEST CASES

No.	APG Input Gases Relative Moles							Equilibrium Exhaust Gases Relative Moles							Surface Reactions (See Table 5)
	H_2*	O_2	CO_2	CO	Ar*	HCl	CF_4	R†	H_2	H_2O	CO	Ar	HCl	HF	
1	1							0	1						1
2	9	4						7	1	8					1,2
3	8	1						2	6	2					1,2,4
4	9		8					20	1	8	8				1,2,3,4
5	2		1					11	1	1	1				1,2,3,4
6	8	1		1				4	6	2	1				1,2,3,4
7	2	1			4			0.2		2		4			2,4
8	2	1		2	4			0.5		2	2	4			2,4
9	10					1		1	10				1		1,5
10	8	1				1		3	6	2			1		1,2,5
11	16	1	2			8		8	12	4	2		8		1,2,3,4,5
12	9		8			1		20	1	8	8		1		1,2,3,4,5
13	12		6			1		12	6	6	6		1		1,2,3,4,5
14	52	7					2	5	36	12	2			8	1,2,3,4,6
15	20	3					2	7	12	4	2			8	1,2,3,4,6
16	11	4	1				1	12	1	8	2			4	1,2,3,4,6
17	16	1					2	4	12		2			8	1,3,4,6
18	18	2	1			4	1	7	12	4	2		4	4	1,2,3,4,5,6

*Arc heated gas

†Mass ratio of plenum injected to arc heated gases (approximate)

TABLE 5. SURFACE REACTIONS

Reaction No.	
1	$2C^* + H_2 \rightarrow 2C_2H_2$
2	$C^* + H_2O \rightarrow H_2 + CO$
3	$C^* + CO_2 \rightarrow 2CO$
4	CO Inhibition
5	HCℓ Inhibition
6	HF Inhibition

to which a particular reactant (or poison) can be isolated and the operating limitations of the APG. Note that the exhaust gas composition is only representative and that all gases that contain CO will also have CO_2 in small quantities. At high temperatures, it is not possible to have large concentrations of CO_2 in the presence of H_2 since the preferred species would be H_2O and CO.

3.2 TEST GAS SELECTION

Of the gases shown in Table 4, those that contain HCℓ and HF require special toxic gas handling systems. The current Aerotherm APG facility is equipped to handle HCℓ, however, a number of nontrivial additions are required before HF can be used. Since it is not at all clear that HF effects are really significant, the current feeling is that a decision on HF testing should be deferred until sufficient motor data with fluorinated propellants becomes available. In the event this data can be analytically treated by an analog between HF and HCℓ then no further APG testing will be necessary. However, should the data not correlate properly, then the expense of the HF handling modifications would be justified. Thus for now, reactions 14 through 18 of Table 4 will be eliminated from consideration.

3.2.1 Test Gas Evaluation

Test gases 1 through 8 have been evaluated under a wide variety of APG conditions using both water cooled calorimeters and carbon test sections. These tests clearly show that test gases 2 and 4 resulted in anomalous heating conditions. The probable cause can be defined by considering the schematic of the APG shown in Figure 1a. In normal operations, H_2 or an inert gas such as N_2, Ar, or He is used as the arc heated column and all other gases are injected between the arc column and the plenum chamber. If we consider, as an example, test gas 2, the relative moles of injection gas (O_2) to arc column gas (H_2) is 4/9. However, mixing of the two gases will be dependent upon the relative mass rates of the two gases. A simple conversion shows that the relative mass of injection gas to arc column gas is approximately 28/1. It was originally anticipated that combustion induced turbulence would result in adequate mixing in the plenum however, measured data suggests a high concentration of low enthalpy injection gases near the walls of the test section. This rather poor mixing of arc heated and injection gases made the test data impossible to adequately analyze. Subsequent trial and error experimentation showed that ratios of injected gas to arc heated gas of less than 5 (by mass) would result in adequate plenum chamber mixing.* Thus test gas number 5 was also eliminated.

*It is assumed that at least one of the injected gases will be O_2 so that there will be combustion induced turbulence.

Experimentation with test gases 4 and 10 revealed a second difficulty. The kinetic reaction rates of CO_2 with H_2 are much slower than those of H_2 with O_2. In fact, some simple kinetic calculations revealed that there was insufficient residence time in the plenum chamber to attain thermochemical equilibrium. Thus, all gases which would normally inject CO_2 would be replaced by an equivalent combination of CO and O_2.

From the above discusssion, HCl test gases 12 and 13 can be eliminated outright, however gas number 11 can be made acceptable by reducing the relative moles of HCl from 8 to 2. Similarly, for the HF gases, gas number 16 can be eliminated and gas numbers 14 and 15 would be more acceptable if relative moles of CF_4 were reduced from 2 to 1. Finally, test gas 9 is unacceptable and needs revision after the effects of HF have been assessed.

3.2.2 Recommended Test Cases for Full Characterization Studies

Based upon the discussion in Section 3.2.1, the test gases for material characterization studies were reduced to the subset shown in Table C. Note that CO_2 will not be used as an injection gas and that it has been replaced by an equivalent quantity of O_2 and CO. Note also that HF gases were not included since the advisability of testing with HF has not yet been assessed.

With the exception of the HF inhibitor all other surface reactants are represented by this set of reactions. It is clearly not possible to isolate reactions other H_2 since oxygen bearing species (CO_2, H_2O) will react with solid carbon to form CO and in gas phase equilibrium, a small quantity of CO_2 will also be present. The reactions shown in Table 5 represent a good compromise between the desire to isolate reactants and still stay within the operating limitations of the APG. In the case of gas mixtures 1, 3, 6, 7, and 8, test samples will be exposed at APG conditions which will result in three nominal surface temperatures, 4000°R, 4500°R and 5500°R. For gas mixtures 2 and 5, samples will be exposed to two nominal surface temperatures, 4000°F and 4500°F; while for gas mixture 4, surface temperature of 4000°R and 5000°F will be used. An inert gas was also included in Table 5 to test for shear removal affects. Inert gas tests will be run at the highest heating conditions compatible with APG limitations. With three tests for five reacting gas mixtures, two tests for three mixtures, and one for the inert gas test, a minimum of twenty-two tests are required. Six additional tests are planned as contingency or repeat tests and will be performed as required. Thus, a total of 28 tests are planned for each characterization material.

TABLE 6. RECOMMENDED MATERIAL CHARACTERIZATION TEST GASES

No.	APG Input Gases Relative Moles					R†	Equilibrium Exhaust Gases Relative Moles					Surface Reactions (see Table 5)
	H_2*	O_2	CO	Ar*	HCℓ		H_2	H_2O	CO	Ar	HCℓ	
1	1					0	1					1
2	2	1		4		0.2		2		4		2,4
3	8	1				2	6	2				1,2,4
4	8	1	1			4	6	2	1			1,2,3,4
5	2	1	2	4		0.5		2	2	4		2,4
6	10				1	1	10				1	1,5
7	8	1			1	3	6	2			1	1,2,3
8	8	1	1		1	5	6	2	1		1	1,2,3,4,5
9				1		0				1		Inert Gas

*Arc heated gas

†Mass ratio of plenum injected to arc heated gases (approximate)

SECTION 4

CALIBRATION TEST RESULTS

Considering the lack of accurate analytical tools for predicting arc heater performance with the various gas mixtures discussed in Section 3.2.2., and the further complication of the very large effect of the plenum/mixing chamber on overall operating efficiency, an effect which would be nearly impossible to model analytically due to the combustion processes occurring in this chamber, a comprehensive series of calibration/checkout tests was run to define the operating limits for each test gas. The following sections describe the results of this test series. Section 4.1 describes the test conditions for each test gas for all gas compositions/heater configurations utilized. Section 4.2 presents the performance map for each test gas while Section 4.3 presents the test nozzle response results of a checkout series run with representative test materials.

4.1 TEST CONDITIONS

Arc heater operation was optimized through a series of calibration/checkout tests using the calibration nozzle assembly to measure cold wall heating rates. Various test gas compositions, combined with different gas injection schemes and arc heater lengths were used to define the maximum run condition possible for that particular test gas. The general criteria for this test series can be summarized as follows:

1. Maximum energy input to test gas
2. Maximum cold wall heating rate
3. Minimum losses in plenum/mixing chamber
4. Maximum test nozzle surface temperature
5. Reasonable arc heater component lifetime
6. Reasonable arc heater running stability

Criteria 1, 2, and 3 generally lead to 4, maximum test nozzle surface temperature; however, it was found that this temperature was a strong function of the gas injection into the plenum chamber. It is felt this is due primarily to mixing and combustion processes in this chamber and their affect on the test section boundary layer. Certain conditions seemed to produce a stratified flow, a very hot core surrounded by a cooler shroud. This produced very low surface temperatures as might be expected.

Since the arc heated or primary gas in most cases was hydrogen, criterion 1 was the easiest to meet within the power supply limitations, the only complicating factor being the unstable running characteristic of arc heating this gas with the present electrode configuration of the arc heater. Criteria 5 and 6 then most often determined the maximum run condition, usually limiting the maximum current that could be reasonably used without seriously degrading arc heater stability and/or lifetime. Various techniques were applied to overcome this limitation as will be described below for each test gas.

Meeting criteria 3, minimum losses in the plenum/mixing chamber, proved to be most difficult. The large size of this chamber, a result of the need to promote complete mixing of the arc heated primary gas with the plenum injected gases, combined with the turbulent nature of the flow in the chamber as induced by the combustion processes and the energy released by these processes, resulted in very large energy losses in this section. Most techniques to control this loss were either inconsistent with the required test conditions, e.g., lower plenum pressure, or adversely affected the flow quality, e.g., smaller plenum chamber. The emphasis therefore was on criteria 1 as discussed above.

The results of the calibration tests are summarized individually for each nominal test gas in Tables 7 through 11. In most cases, the table is arranged in the sequence in which the runs were actually made, showing the effect of test gas composition, gas injection or arc heater configuration changes.

Test Gas 1

Hydrogen is the basic arc heated species for this test series and as such test gas 1 represents the baseline performance for all the test gases. One basic arc heater length was used for all test points shown in Table 7; this selection was based on previous experience with hydrogen. This left the mass flow rate and injection configuration as the only variables available for changing arc heater operation. The injection configuration was held constant, all flow being arc heated, as this produced the highest efficiencies and there were no other reasons for trying different configurations, e.g., gross arc instabilities or component failures.

Several different mass flow rates were tried, with the result that a maximum of 0.007 lbm/sec was found to be acceptable from an operational viewpoint. Higher flow rates resulted in higher chamber pressures with attendant higher heating rates (or recovery temperatures) demonstrating the need for the largest mass flow possible. This flow rate also produced the high arc voltages necessary to lower the arc current to acceptable levels, those which optimize electrode lifetime considering the severity of the test condition. Note that the last three points in Table 7 are the nominal test points for test gas 1.

TABLE 7. TEST GAS 1 CALIBRATION RESULTS

Test	Enthalpy H_o (Btu/lbm)	Chamber Pressure P_c, (atm)	Recovery Temperature T_r, (°R)	Cold Wall Heating Rate $\dot{q}_{cw}$(Btu/ft²sec)	Flow Rate $\dot{m}$ (lbm/sec)	Test Gas Composition (Relative Moles/Mass Fraction)				Symbol	Arc Voltage (Volts)	Arc Current (amps)	Effic (%)
						H_2	Ar	O_2	CO				
2439,02	31,540	1.90	5820	–	0.00431	1.0/1.0					(810)	500	35.4
2439,04	34,390	2.20	5990	1200	0.00452	1.0/1.0					(850)	590	32.7
2453,01	36,880	3.80	6270	1172	0.00695	1.0/1.0					929	852	34.3
2453,02	33,250	3.80	6090	1090	0.00695	1.0/1.0					911	784	34.1
2453,03	36,040	3.90	6240	1240	0.00695						923	892	32.1
2454,01	33,970	3.80	6130	832	0.00695	1.0/1.0					917	780	34.8
2457,01	49,780	4.30	6810	1160	0.00695	1.0/1.0					977	1206	31.0
2458,01	33,030	3.60	6060	787	0.00695	1.0/1.0					915	750	35.3
2459,01	44,840	4.05	6610	996	0.00695	1.0/1.0					952	978	35.3
2583,03	51,420	4.08	6840	1050	0.00704	1.0/1.0					1012	918	41.1
*2583,04	41,900	3.78	6480	829	0.00704	1.0/1.0					981	724	43.8
*2583,05	53,690	4.28	6930	1204	0.00704	1.0/1.0					1050	953	39.8
*2583,06	64,200	4.59	7280	1562	0.00704	1.0/1.0					1089	1178	37.2
*Nominal Test Points													

TABLE 8. TEST GAS 2 CALIBRATION RESULTS

Test	Enthalpy H_o (Btu/lbm)	Chamber Pressure P_c, (atm)	Recovery Temperature T_r, (°R)	Cold Wall Heating Rate $\dot{q}_{cw}$(Btu/ft²sec)	Flow Rate $\dot{m}$ (lbm/sec)	Test Gas Composition (Relative Moles/Mass Fraction)				Symbol	Arc Voltage (Volts)	Arc Current (amps)	Effic (%)
						H_2	Ar	O_2	He				
2438,01	950	5.80	6190	3000	0.0332	2.2/ 0.122		0.1/ 0.878		▽	(1110)	510	5.80
2469,01	1560	5.90	6320	1277							1005	619	8.80
2470,01	1660	6.10	6240	1125							1004	618	9.40
2470,02	5060	6.20	6910	1358							1358	820	18.2
2503,01	2860	6.20	6570	1202							927	835	12.9
2612,01	2850	4.72	6960	754	0.0299	2.1/ 0.033	2.3/ 0.717	1./0/ 0.250		⊙	647	1008	13.7
2612,01	3180	5.07	7120	768							644	1210	12.9
2612,02	3700	5.25	7330	761							648	1521	11.9
2600,01	2510	5.62	6690	1218	0.0384	2./ 0.055	0.94/ 0.510	1./ 0.435		⊡	883	683	16.8
2600,02	2620	6.11	6750	1326							909	893	13.1
2600,03	2680	6.38	6780	1484							952	977	11.7
2608,01	2410	6.23	6700	1208	0.0398	2./ 0.053	1./ 0.525	1./ 0.422			856	795	14.9
2608,02	2940	6.66	6890	1436							917	1006	13.5
2608,03	3790	6.84	7140	1516							933	1208	14.1

TABLE 8. (CONCLUDED)

Test	Enthalpy H_o (Btu/lbm)	Chamber Pressure P_c, (atm)	Recovery Temperature $T_{r'}$ (°R)	Cold Wall Heating Rate $\dot{q}_{cw}$(Btu/ft²sec)	Flow Rate $\dot{m}$ (lbm/sec)	Test Gas Composition (Relative Moles/Mass Fraction)				Symbol	Arc Voltage (Volts)	Arc Current (amps)	Effic (%)
						H_2	Ar	O_2	He				
2599,01	144	10.56	957	889	0.0762	2.2/ 0.057	0.93/ 0.479	1./ 0.413	0.99/ 0.051	◿	450	795	3.25
2599,02	337	10.72	1218	980							476	1005	5.68
2599,03	549	10.90	1537	1049							502	1210	7.27
2606,01	407	10.76	1320	1056							443	790	9.3
2606,01	661	11.34	1714	1069							476	1000	11.2
2606,01	869	11.54	2054	1094							505	1209	11.5
2610,01	1970	7.38	7070	909	0.0584	2.1/ 0.017	5.4/ 0.856	1./ 0.127		△	724	1010	16.5
2610,01	2210	8.04	7260	949							731	1216	15.4
2610,01	1570	7.87	6750	872							722	793	16.9
2614,01	2332	8.28	7380	1038	0.0597	2.2/ 0.017	5.5/ 0.858	1./ 0.125			740	1425	14.0
2613,01	2830	7.30	7510	959	0.0497	2.1/ 0.020	4.4/ 0.829	1./ 0.151		◇	722	1422	14.4
*2616,01	2270	7.02	7130	919							709	1007	16.6
*2616,03	2590	7.11	7350	990							712	1419	13.5
*Nominal Test Points													

TABLE 9. TEST GAS 3 CALIBRATION RESULTS

Test	Enthalpy H_o (Btu/lbm)	Chamber Pressure P_c, (atm)	Recovery Temperature $T_{r,s}$ (°R)	Cold Wall Heating Rate $\dot{q}_{cw}$ (Btu/ft²sec)	Flow Rate $\dot{m}$ (lbm/sec)	Test Gas Composition (Relative Moles/Mass Fraction)				Symbol	Arc Voltage (Volts)	Arc Current (amps)	Effic (%)
						H_2	Ar	O_2	CO				
2460,01	7030	6.10	5980	1210	0.0222	7.9/ 0.333		1./ 0.667			1049	759	22.9
2461,01	12,150	6.73	6750	2400							813	712	24.9
2462,01	10,830	5.63	6613	1741							1114	1316	22.4
2464,01	11,280	7.10	6740	1910							1159	1027	22.5
2465,01	6,940	5	6680	1234							1039	617	25.3
2466,01	7,230	5.02	6930	1428							1042	627	27.0
2467,01	8,960	6.75	6400	1692							1063	809	23.9
2486,04	12,670	7.42	6920	2491							1218	1005	24.2
2487,01	3,060	6.0	4550	1543							1182	575	31.2
2587,02	10,850	7.71	6422	2423							1225	761	27.3
2587,03	13,690	7.[illegible]	6940	3097							1305	961	25.6
*2588,01	8,420	6.37	7220	1563							1200	563	29.2
*2588,02	11,500	6.[illegible]	6730	2298							1288	740	28.2
*2588,03	11,900	7.41	7040	2830							1295	956	28.2
*Nominal Test Points													

TABLE 10. TEST GAS 4 CALIBRATION RESULTS

Test	Enthalpy H_o (Btu/lbm)	Chamber Pressure P_c, (atm)	Recovery Temperature T_r, (°R)	Cold Wall Heating Rate $\dot{q}_{cw}$(Btu/ft²sec)	Flow Rate $\dot{m}$ (lbm/sec)	Test Gas Composition (Relative Moles/Mass Fraction)				Symbol	Arc Voltage (Volts)	Arc Current (amps)	Effic (%)
						H_2	Ar	O_2	CO				
2490,01	7330	6.80	6620	1534	0.0269	7.8/ 0.220		1./ 0.447	0.85/ 0.332		1207	807	21.4
2492,01	4650	6.30	6100	1414							1144	638	20.2
2493,01	5610	6.50	6310	1671							1152	736	20.6
2595,01	7000	7.20	6570	1960	0.0271	7.9/ 0.223		1./ 0.448	0.84/ 0.330		1295	599	27.6
*2595,02	6680	7.35	6520	1834							1296	608	26.3
*2595,03	7150	7.53	6610	2112							1332	668	23.7
*2595,04	7410	7.78	6660	2116							1310	759	22.9
*Nominal Test Points													

TABLE 11. TEST GAS 5 CALIBRATION RESULTS

Test	Enthalpy H_o (Btu/lbm)	Chamber Pressure P_c, (atm)	Recovery Temperature T_{R_2} (°R)	Cold Wall Heating Rate $\dot{q}_{cw}$(Btu/ft² sec)	Flow Rate $\dot{m}$ (lbm/sec)	Test Gas Composition (Relative Moles/Mass Fraction)				Symbol	Arc Voltage (Volts)	Arc Current (amps)	Effic (%)
						H_2	Ar	O_2	CO				
2604,01	2230	6.31	6860	.236	0.0402	2./ 0.038	1./ 0.385	1./ 0.306	1./ 0.271	○	859	1000	13.2
2611,01	1570	9.19	6900	1080	0.0714	1./ 0.014	2.5/ 0.701	0.82/ 0.182	0.53/ 0.103	◇	771	1210	15.2
2611,02	1300	9.32	6700	953							776	1010	15.4
2611,03	1120	9.24	6540	987							771	791	17.6
2618,01	1530	8.40	6920	1026	0.0629	2.1/ 0.016	4.4/ 0.655	1./ 0.119	2./ 0.210	□	752	1215	12.2
*2618,02	1640	8.41	7010	1046							746	1417	14.5
*2620,01	1090	8.36	6570	974							787	738	16.4

*Nominal Test Points

Test Gas 2

Referring to Table 8, a large range of test gas compositions and injection configurations were tried before achieving an acceptable balance between test gas recovery temperature, chamber pressure and arc heater operation. In early tests, it was found that injection of large amounts of oxygen, in relation to the primary hydrogen flow, into the plenum chamber had adverse effects on the arc stability to the point of driving the arc termination at the anode (nearest the plenum) upstream into the constrictor column. This usually resulted in early failure of the column segments. The solution to this problem was to inject varying amounts of an inert carrier (Argon) along with the hydrogen primary flow to force the arc termination into the proper location on the anode, while at the same time reducing the oxygen flow to the plenum. This necessitated a reduction in the hydrogen flow to maintain the desired molar concentrations.

Several tests (2599-2506) were run with a completely inert primary flow of Argon/Helium, adding all the reactants in the plenum. This resulted in very smooth, stable arc operation but with very low arc voltage. As the arc current is limited, primarily by the electrode design and secondarily by the power supply characteristics, very low test gas enthalpies and hence low recovery temperatures were achieved. The net result was that while measured cold wall heating rates were quite high, achievable test nozzle surface temperature would be severely limited. For this reason, this particular gas composition was abandoned.

The resulting test points for test gas 2 are the two final points of Table 8.

Test Gas 3

Unlike test gas 2, the primary flow of hydrogen for test gas (see Table 9) was adequate for the relatively small amount of oxygen injected in the plenum. The primary effect of the oxygen injection in this case was an increase in the instability of the arc operation limiting maximum arc current to significantly lower levels. Efforts were therefore focused on increasing arc voltage through changes in the oxygen injection configuration to maintain total energy input to the test gas at the maximum level.

The final three points shown in Table 9 are the nominal test conditions for test gas 3.

Test Gas 4

Test Gas 4 is similar to test gas 3 with the addition of carbon monoxide injected in the plenum. The total mass flow is increased with a resulting increase in arc voltage and accompanying decrease in overall efficiency.

The last three points shown in Table 10 are the nominal test conditions for this test gas. Note that a performance limit appears to have been reached around the 660 amp arc current level, further increases in arc current producing only slightly higher recovery temperatures. For this reason, there may be effectively only two test conditions for test gas 4.

Test Gas 5

Test Gas 5 is similar to test gas 2 with the addition of carbon monoxide injected in the plenum. The primary effect is again an increase in arc voltage. There is little change in the arc stability, allowing the same maximum current level as used for test gas 2 to be used, thus increasing the power input to the test gas and overcoming somewhat the cooling effect of the increased mass flow. The final results are shown in Table 11.

4.2 PERFORMANCE MAPS

The calibration data of Tables 7 through 11 are presented in graphical form as performance maps in Figures 13 through 17. The average bulk enthalpy, H_o, is plotted against the total gas flow rate, $\dot{m}$, divided by the APG sonic area, A*, (nozzle throat area) and the chamber pressure, P_c. The curve noted on the map is the best fit for the limited data available for a particular test gas composition.

The various test gas compositions used for test gas 2 can be realistically divided into four distinct compositions yielding four curves. In the case of test gas 5, none of the three compositions used yielded sufficient data for accurate curve fitting.

4.3 TEST NOZZLE RESPONSE

As a final calibration effort, a checkout series of tests were run at the highest test condition for each test gas with three representative materials, c-plane P.G., ATJ graphite and P03 graphite. The measured peak surface temperatures for this series is detailed in Table 12.

The test nozzle response in each case is presented in Table 13. The analytical and/or source of each item in this table are detailed in Appendix A, APG Data Analysis Procedures.

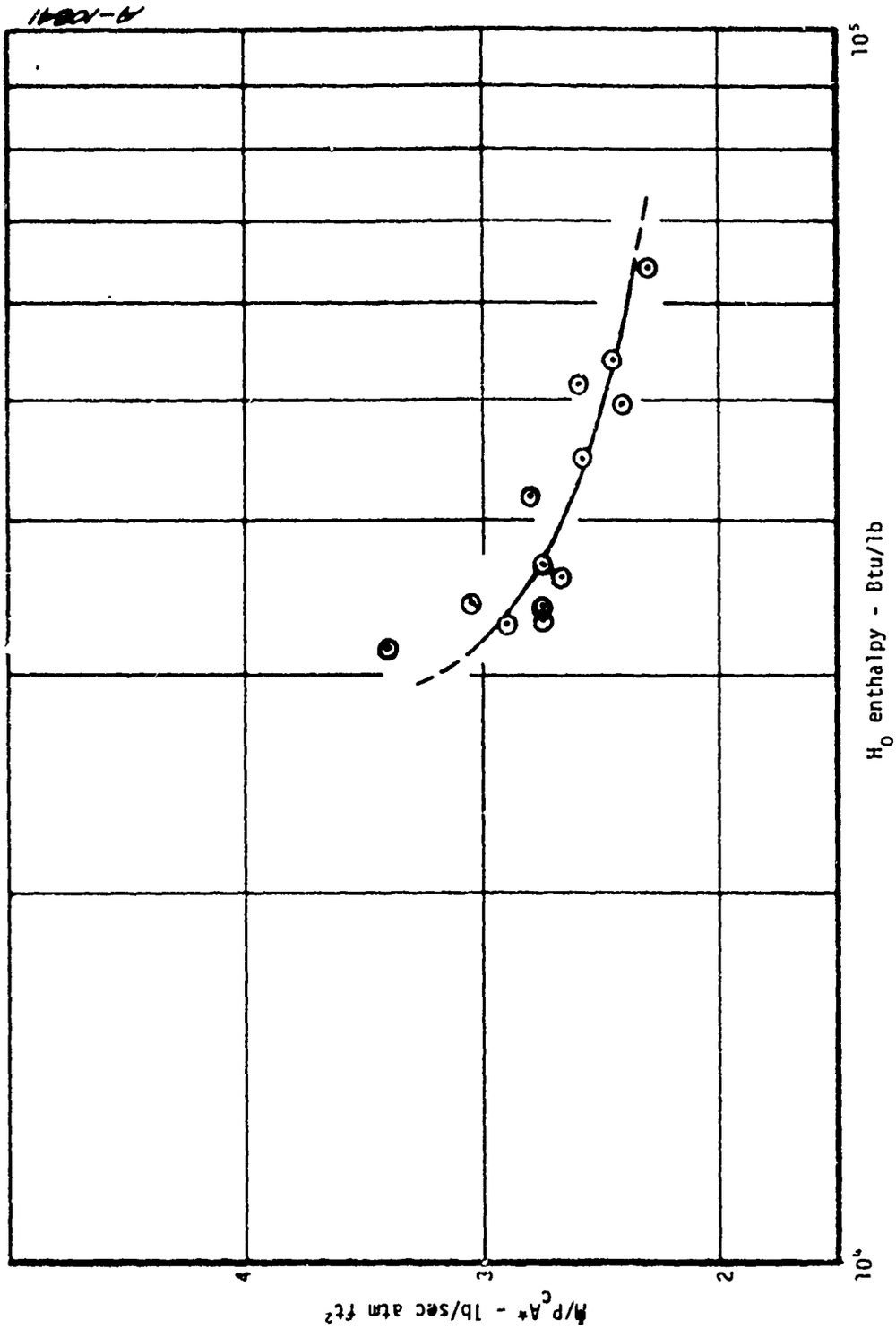

Figure 13. Performance map, test gas 1.

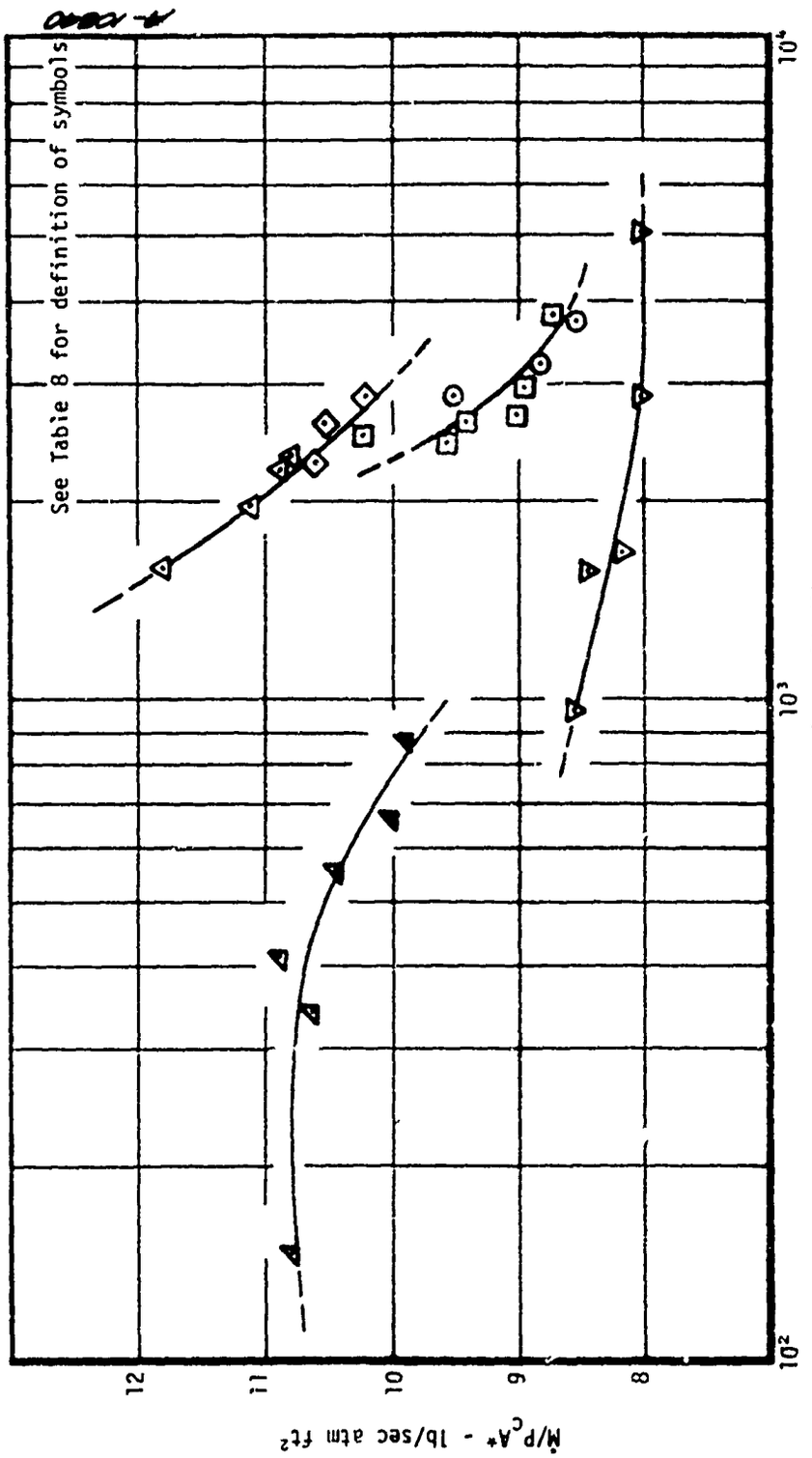

Figure 14. Performance map, test gas 2.

Figure 15. Performance map, test gas 3.

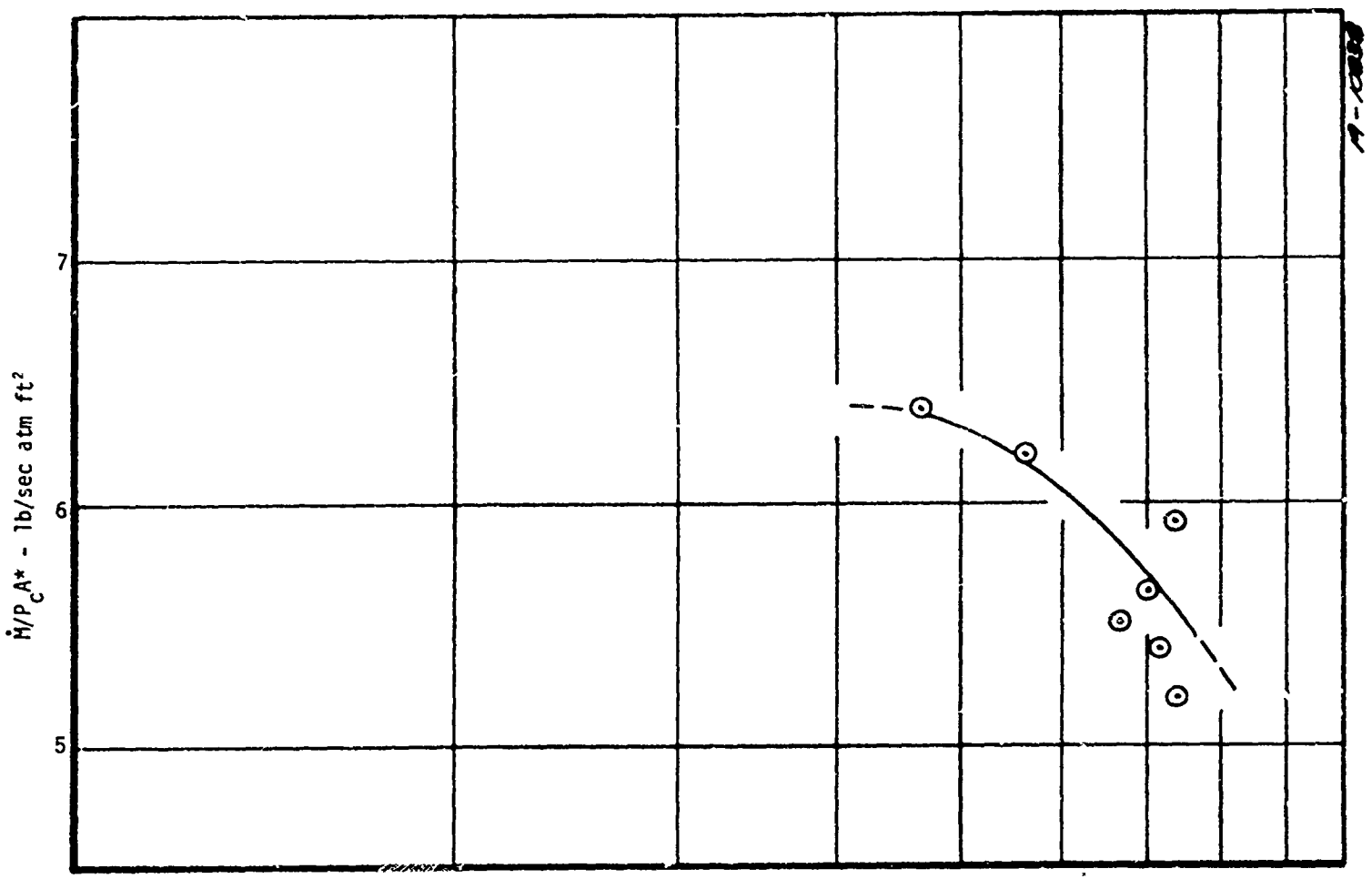

Figure 16. Performance map, test gas 4.

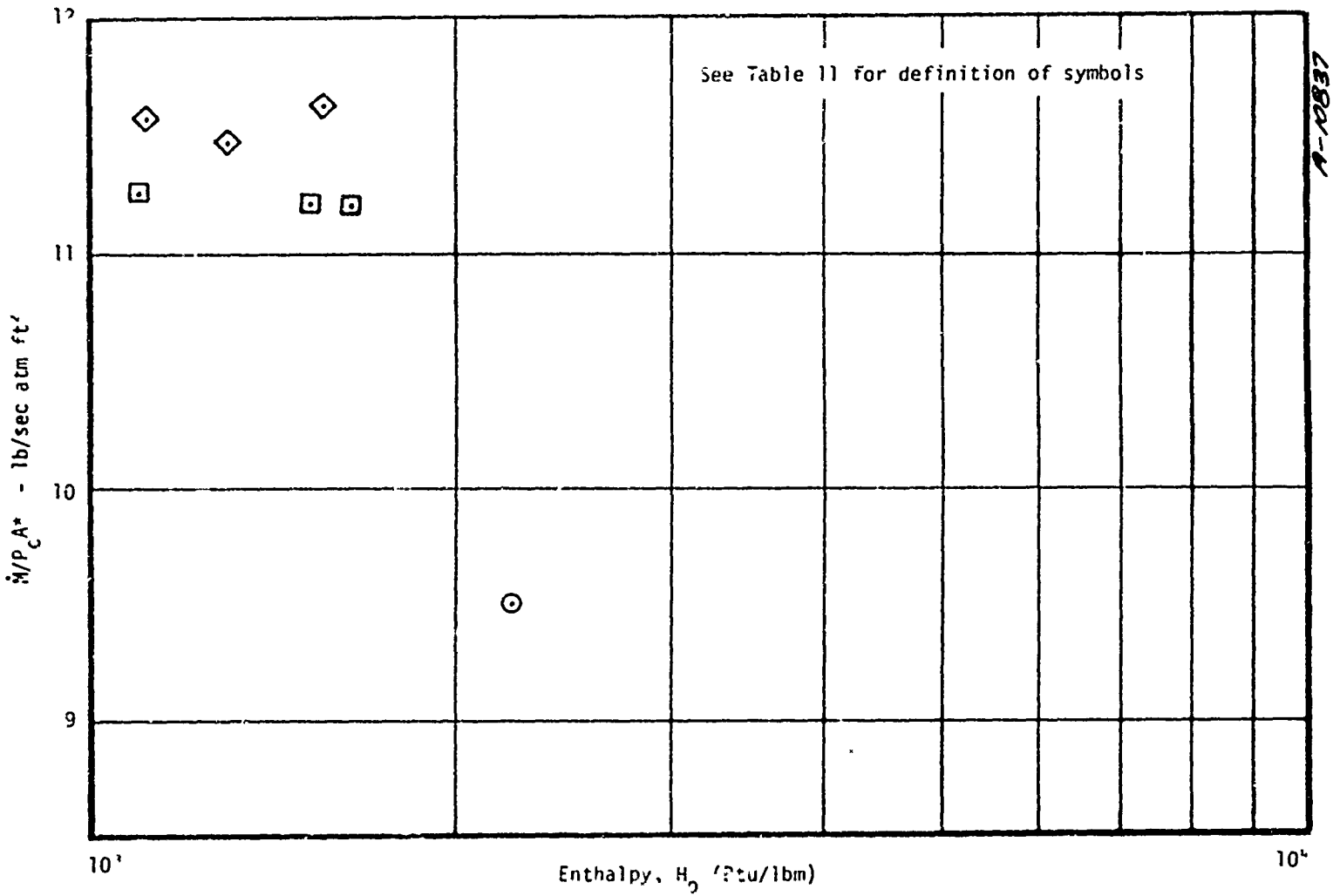

Figure 17. Performance map, test gas 5.

TABLE 12. PRELIMINARY TEST RESULTS, SURFACE TEMPERATURE COMPARISON, HIGHEST TEST CONDITION

Test Gas	Surface Temperature (°R)			Calibration Test
	C-Plane PG	PO3 Graphite	ATJ Graphite	
1	5220	5190	5040	2583,06
2	4540	4270	3970	2616,03
3	5120	5080	4840	2588,03
4	5100	—	4760	2595,04
5	—	—	4030	2618,01

TABLE 13. CHECK OUT TEST SERIES, TEST NOZZLE RESPONSE

Test	Test Gas	Material	Plenum State			Edge State		Cold Wall Heat Rate, $\dot{q}_{cw}$ (Btu/ft²sec)	Transfer State		Average Surface Recesssion (inch)	Mass Removal Rate, $\dot{M}_c$ (lbm/ft²sec)	B'_{meas}	Average Surface Temperature, T_w (°R)	$B'_{diffusion}$	$B'/B'_{diffusion}$
			Enthalpy, H_o (Btu/lb)	Chamber Pressure, P_c (atm)	Recovery Temperature, T_r (°R)	Pressure, P_e (atm)	Temperature, T_e (°R)		Heat Transfer Coefficient $\rho_e u_e C_H$	Mass Transfer Coefficient $\rho_e u_e C_m$ (lbm/ft²sec)						
2586.01	1	C-Plane PG	65,400	4.44	7301	2.54	6907	1562	0.0515	0.0213	0.0145	2.00-03	0.0339	5150	0.4036	0.2327
2385,03	1	PO3 Graphite	62,200	4.65	6637	2.66	6284	1562	0.0553	0.0228	0.00954	1.487-03	0.0652	5150	0.4020	0.1622
2593,01	1	ATJ Graphite	55,133	4.23	6975	2.42	6607	1204	0.0508	0.0236	0.00438	3.75-04	0.0377	4850	0.1916	0.1935
2617,05	2	C-Plane PG	2,633	6.36	6899	3.66	6566	990	0.2750	0.1450	0.00933	1.65-03	0.0113	4400	0.2570	0.0443
2617,02	2	PO3 Graphite	2,682	6.29	6912	3.62	6579	990	0.2742	0.1452	0.03917	6.63-03	0.0457	4000	–	–
2617,01	2	ATJ Graphite	2,925	6.08	6986	3.50	6647	990	0.2684	0.1409	0.03925	6.95-03	0.0493	3800	0.2531	0.2097
2592,04	3	C-Plane PG	16,600	6.89	7134	3.96	6786	2830	0.1521	0.0968	0.060	1.10-02	0.1136	4750	0.4717	0.2408
2592,02	3	PO3 Graphite	16,350	6.74	7105	3.87	6760	2830	0.1487	0.0946	0.0390	8.39-03	0.0887	4950	0.5165	0.1717
2592,01	3	ATJ Graphite	16,700	6.68	7129	3.84	6781	2830	0.1484	0.0945	0.0528	1.00-02	0.1061	4750	0.4720	0.2248
2597,02	4	C-Plane PG	9242	6.82	7367	3.92	6524	2116	0.1825	0.0992	0.0480	7.63-03	0.0769	4950	0.3918	0.2014
2597,01	4	ATJ Graphite	9300	6.81	7373	3.92	6531	2116	0.1841	0.1002	0.0443	7.117-03	0.0710	4650	0.3393	0.2092
2619,01	5	ATJ Graphite	1798	7.54	7021	3.66	6619	1026	0.2256	0.1767	0.0347	1.09-02	0.0617	4000	0.1026	0.6014

SECTION 5

SUMMARY AND CONCLUSIONS

The process for selecting test gases and test conditions for arc plasma generator simulation of propellant environments was described. By considering the important reactants, anticipated environmental conditions, the sensitivity of surface kinetics to these conditions, and arc plasma operating limitations, a set of test gases was selected. Each of the test gases has been subjected to extensive calibration and checkout runs to define anticipated surface heating rates and temperatures for graphitic materials. These gases permit a separation of the effects of various reactants so that materials tested with these gases can be analyzed and correlated to yield kinetic reaction rates which are appropriate for rocket nozzle environments.